



January 2023

Deep Geothermal Wells: Enhancing The Suitability Of High-Density-Water-Based Drilling Mud To Sustain Harsh Subsurface HP/HT Gradients.

Opeyemi Olaolu Oni

[How does access to this work benefit you? Let us know!](#)

Follow this and additional works at: <https://commons.und.edu/theses>

Recommended Citation

Oni, Opeyemi Olaolu, "Deep Geothermal Wells: Enhancing The Suitability Of High-Density-Water-Based Drilling Mud To Sustain Harsh Subsurface HP/HT Gradients." (2023). *Theses and Dissertations*. 5688. <https://commons.und.edu/theses/5688>

This Thesis is brought to you for free and open access by the Theses, Dissertations, and Senior Projects at UND Scholarly Commons. It has been accepted for inclusion in Theses and Dissertations by an authorized administrator of UND Scholarly Commons. For more information, please contact und.commonson@library.und.edu.

DEEP GEOTHERMAL WELLS: ENHANCING THE SUITABILITY OF HIGH-DENSITY-WATER-BASED DRILLING MUD TO SUSTAIN HARSH SUBSURFACE HP/HT GRADIENTS.

By

Opeyemi Oni

Bachelor of Engineering, University of Port Harcourt, Port Harcourt, Nigeria. 2016

A Thesis

Submitted to the Graduate Faculty

of the

University of North Dakota

In partial fulfillment of the requirements

for the degree of

Master of Science in Geology

Grand Forks, North Dakota

December

2023

Name: Opeyemi Oni

Degree: Master of Science

This document, submitted in partial fulfillment of the requirements for the degree from the University of North Dakota, has been read by the Faculty Advisory Committee under whom the work has been done and is hereby approved.

DocuSigned by:
William Gosnold
9C5B71FF939D427...
William Gosnold

DocuSigned by:
Adesina Fadairo
902E574CDE9C40D...
Adesina Fadairo

DocuSigned by:
Dongmei Wang
1DB75A6E288A402...
Dongmei Wang

This document is being submitted by the appointed advisory committee as having met all the requirements of the School of Graduate Studies at the University of North Dakota and is hereby approved.

DocuSigned by:
Chris Nelson
3E0AF088C733403

Chris Nelson

Dean of the School of Graduate Studies

9/29/2023

Date

PERMISSION

Title: Deep Geothermal Wells: Enhancing the Suitability of High-Density-Water-Based Drilling Mud to Sustain Harsh Subsurface HP/HT Gradients.

Department: Harold Hamm School of Geology and Geological Engineering

Degree: Master of Science

In presenting this thesis in partial fulfillment of the requirements for the graduate degree from the University of North Dakota, I agree that the library of the University shall make it freely available for inspection. I further agree that permission for extensive copying for scholarly purposes may be granted by the professor who supervised my thesis work or, in his absence, by the Chairperson of the department or the Dean of the School of Graduate Studies. It is understood that any copying or publication or other use of this thesis or part thereof for financial gain shall not be allowed without my written permission. It is also understood that due recognition shall be given to me and to the University of North Dakota for any scholarly use which may be made of any material in my thesis.

Opeyemi Oni

September 29, 2023

ABSTRACT

The harsh temperature in which some reservoirs are geologically located has presented a major drilling fluids challenge to the geothermal industry. Therefore, the design of drilling fluid that will be effective and cost-friendly in high-temperature high-pressure (HPHT) environments has become an age-long threat to the economic development of geothermal resources. A geothermal drilling fluid should possess high thermal stability while performing the basic functions of drilling fluid all through the drilling process. Exerting sufficient hydrostatic pressure, suspension, and effective removal of cuttings, shale stabilization, minimum filtrate loss, and thin filter cake thickness. Ilmenite was adopted as a weighting material due to its advantages over barite. This study evaluates the effectiveness of fly ash buffered with an industrial standard copolymer to eliminate ilmenite sag, filtrate loss, and rheological instability encountered with ilmenite-densified water-based drilling fluids at HPHT environments when accessing geothermal wells. Four laboratory barrels of water-based drilling fluids were formulated for this study. Fly ash of 130 μm particle size was added to mud samples at 0, 1, 2, and 3 lb./bbl ratios. The influence of fly ash on drilling fluids properties was thoroughly evaluated by measuring static and dynamic sagging at vertical and inclined (30° , 45° , 60° , 70° , 80° , and 90°) conditions over a range of temperatures (250°F , 300°F , 350°F , and 400°F). A high sag factor (SF) occurs between 45° - 75° , with 61° as the peak regardless of the temperature alteration. Additionally, it was observed that the inclusion of fly ash improves the sagging phenomena, the rheological and filtration behavior of the water-based mud samples to satisfy the industrial API standard value.

Table of Contents

PERMISSIONiii

ABSTRACT.....1

LIST OF FIGURES.....3

LIST OF TABLES.....4

CHAPTER I.....5

INTRODUCTION.....5

 1.0 Difficulties of Geothermal Well Drilling Fluid7

 1.1 The Importance of Rheological Properties.....8

 1.2 The Factors Affecting Drilling Mud Flow Properties.....9

 1.3 The Challenges of Rheological Properties.....10

 1.4 A Field Challenge of Sag Phenomenon.....12

CHAPTER II – LITERATURE REVIEW.....14

 2.0 Geothermal Wells in the United States.....14

 2.1 Geothermal Well Drilling Fluid System.....14

CHAPTER III – METHODOLOGY.....19

3.0 Materials.....	19
3.1 Drilling Fluid Sample Preparation.....	27
3.2 Drilling Fluid Properties Measurement.....	30
CHAPTER IV – RESULTS AND ANALYSIS.....	37
4.0 Sagging Efficiency.....	37
4.1 Rheology.....	50
4.2 Filtration Loss.....	53
CHAPTER V – CONCLUSION.....	56
REFERENCES.....	58

LIST OF FIGURES

Figure 1. The Geothermal Resources of the United States	6
Figure 2. The comparison between both geothermal and oil well drilling	8
Figure 3. The Schematic of a Sag Phenomenon	11
Figure 4. The Deposition of Cuttings Bed.....	12
Figure 5. The Experimental Flowsheet.....	19
Figure 6. Location of fly ash and ilmenite.....	20
Figure 7. Stack of Sieves	22
Figure 8. The Sieve Shaker.....	22
Figure 9. The Particle Size Distribution of Samples	24
Figure 10. Scanning Electron Microscopy of ilmenite	25
Figure 11. Scanning Electron Microscopy of ilmenite	26
Figure 12. The XRD result of Fly Ash	27
Figure 13. A Multimixer Machine	30
Figure 14. The Sagging Test Equipment.....	33
Figure 15. A Mud Balance.....	33
Figure 16. An 8-Speed Viscometer.....	35
Figure 17. A High-Pressure High-Temperature Filter Press	36

Figure 18. Static Sag Test for Base Mud	39
Figure 19. Static Sag Test for Base Mud at 0 ⁰ , and 45 ⁰	40
Figure 20. Static Sag Test for Base Mud Plus 3 lb./bbl of Fly Ash	42
Figure 21. Static Sag Test for Base Mud at 0 ⁰ , 45 ⁰ , and 60 ⁰	43
Figure 22. Dynamic Sag Test for Base Mud Plus 0 and 3 lb./bbl of Fly Ash	45
Figure 23. Static Sag Results Comparison.....	46
Figure 24. Dynamic Sag Results Comparison.....	47
Figure 25. The Schematic of a Sag Phenomenon	50
Figure 26. The Effect of Fly Ash on Plastic Viscosity.....	51
Figure 27. The Effect of Fly Ash on Yield Point	51
Figure 28. The Effect of Fly Ash on 10 S Gel	53
Figure 29. The Effect of Fly Ash on 10 Min Gel.....	54
Figure 30. The Filtrate Loss of Base Mud Plus Fly Ash	54
Figure 31. The Filter Cake Thickness of Base Mud Plus Fly Ash	55

LIST OF TABLES

Table 1. The X-Ray Diffraction Analysis Results for Fly Ash.....	6
Table 2. Composition of a Drilling Fluid Barrel.....	28
Table 3. Data of Static Sag for Base Mud at Inclined Angles.	39
Table 4. Data of Static Sag for Base Mud Plus Fly Ash.....	42
Table 5. Relationship between inclination and setting	49

CHAPTER I

INTRODUCTION

Geothermal reservoirs are regarded as a magnificent green energy source because of the increased demand for electricity and the developing environmental problems related to the oil sector. As a result, there have been a lot more geothermal drilling and exploring initiatives during the past few decades to gain access to geothermal reservoirs (Kiran and Salehi, 2020). Geothermal resources can be harnessed by drilling wells into the geothermal reservoir to produce the earth's heat to the surface (Finger and Blankenship, 2010). Oil well drilling is almost the same as drilling for a geothermal well but with the involvement of high temperatures (Bavadiya et al., 2019; Teodoriu., 2019). To the best of my knowledge, no known standards are applicable for drilling geothermal resources yet, but HPHT oil and gas reservoirs exhibit close characteristics with geothermal reservoirs. For this reason, the inventions made in drilling fluid technology for drilling oil and gas reservoirs could be applicable to drilling geothermal reservoirs (Teodoriu et al., 2018). Hence, technical challenges encountered in geothermal well drilling and completions may be tackled with the application of the knowledge of oil and gas well drilling and completions. Oftentimes, geothermal reservoir temperature may exceed oil and gas reservoir temperature. However, both reservoir fluids show huge dissimilarities and the geological location of geothermal resources is usually harsh.

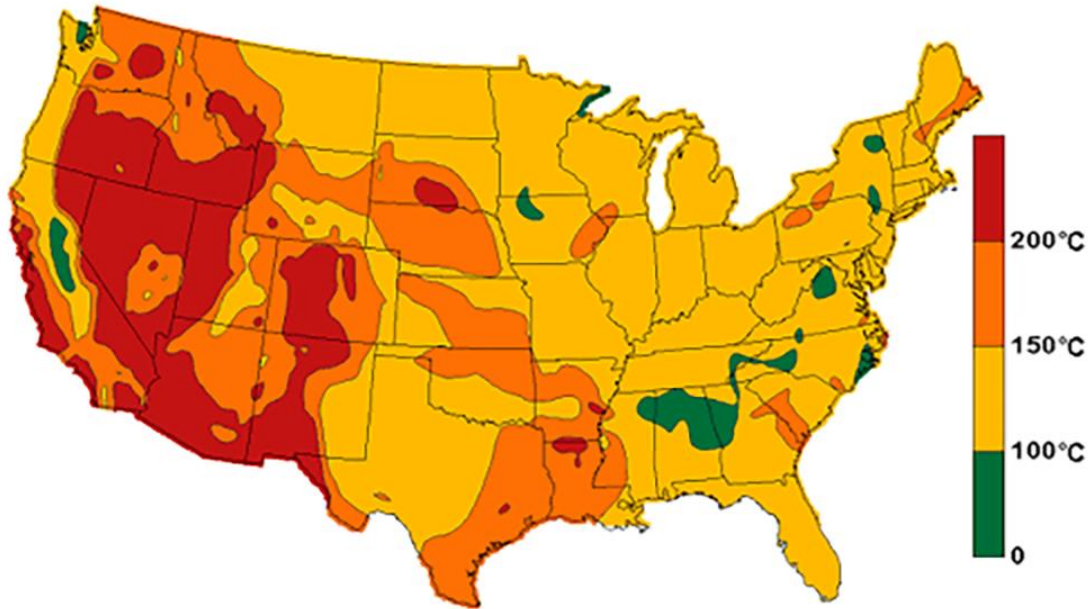


Figure 1. The Geothermal Resources of the United States. (Source: U.S. Department of Energy)

Geothermal resources may be subdivided into three divisions according to the temperature of their geological environment: the lower-temperature reservoir (below 150⁰C), the medium-temperature reservoir (within 150⁰C and 200⁰C), and the high-temperature reservoir (above 200⁰C) (Kruszewski and Wittig, 2018). Deductively, the temperature of some geothermal reservoirs may go beyond the critical temperature of the water, posing significant jeopardy to the drilling and completion of geothermal wells. Therefore, the materials for the design of geothermal drilling fluids must be carefully selected to withstand HPHT conditions. Figure 1 highlights the distribution of geothermal resources in the United States.

1.0 Difficulties in drilling fluid technology for geothermal well drilling

Consequent to the HPHT conditions of the location of geothermal resources, specially selected drilling fluid additives are encouraged for application in geothermal drilling fluid design. The additives must be able to resist the harsh downhole environment in which geothermal reservoirs geologically occurred. Failure of the drilling fluid to meet this requirement could lead to difficulties as a result of thermal degradation. This process is technically complicated due to the severe circumstances, which combine elevated temperatures with hard, very abrasive rock in an environment of corrosive fluids. Greywacke, quartzite, granite, and granodiorite are examples of volcanic rocks that are frequently found as formation rocks in geothermal reservoirs.

Additionally, the high cost of drilling fluid for drilling geothermal wells is a concern. A study of both 21 geothermal wells and 21 oil and gas wells was investigated. As observed in Figure 2, the study compares depth with operational time for the same operation scenario, and the results suggested that there was a huge difference in the number of days taken to complete a geothermal well compared to an oil well. This is an indication of the challenges encountered in terms of cost; labor cost, drilling fluid services, and daily rig rate in geothermal drilling (Vivas et al., 2020). The drilling activities cost for a geothermal well is usually around 40-60% of the project's total cost irrespective of the complications encountered while drilling a geothermal well (Bavadiya et al., 2019).

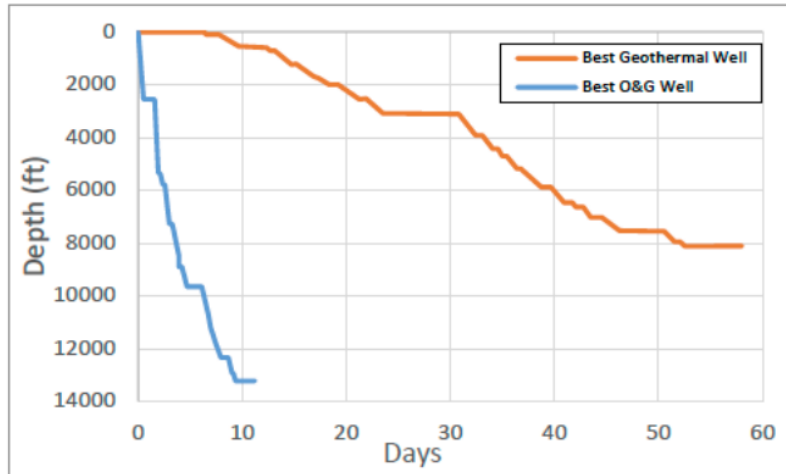


Figure 2. Comparison between both geothermal and oil well drilling (Vivas et al., 2020).

1.1 The importance of drilling fluid’s rheological properties in geothermal well drilling

The success of a drilling operation is significantly determined by the rheological properties of the mud (Chemwotei, 2011). Drilling fluids perform ten (10) basic functions during a drilling operation as; transporting freshly cut cuttings to the surface, providing sufficient hydrostatic pressure for the mud column, lubricating and cooling the drill stem, enhancing wellbore stability etc, (Fadairo et al., 2017; Oni et al., 2023). A thorough investigation of additives’ properties is necessary to select an optimum combination of additives that will be suitable to perform the functions stated above, especially in environments of elevated temperature (Mohamed et al., 2021). The flow characteristics of drilling mud have a notable impact on many drilling parameters such as; drilling mud stability, the thickness of the filter cake, drill bit penetration speed, hole hydraulics, and wellbore cleaning (Elkatatny, 2019). Lost circulation has been identified by previous researchers as a rheological property dependent (Kulkarni et al., 2013). The impact of lost circulation in cavernous zones may be overcome by increasing the mud’s shear rate. This

outcome is also applicable to geothermal reservoirs because they are characterized by naturally fractured formations (Magzoub et al., 2021).

1.2 Factors that affect drilling mud flow properties in geothermal drilling.

Periodic information about the effect of the downhole environment on drilling mud is necessary throughout the drilling activities. The changes in the properties of drilling mud are highly discouraged for cost-friendly and successful geothermal well drilling. Despite being popularly drilled with bentonite water-based mud a noticeably higher yield stress was reported at high temperature. High temperature-induced flocculation and swelling of the clay as well as sodium ions' replacement may be responsible for high-yield stress increment (Ahmad et al., 2018).

High temperatures also destroy polymeric compounds used in drilling fluid, which lowers the viscosity of the mud and reduces its efficiency, ultimately making drilling operations more difficult (HPHT recent papers). Additionally, elevated pressure also alters the volume of the continuous phase due to compression, raising the viscosity of oil-based drilling muds (Amani and Al-Jubouri, 2012).

The changes in the chemical makeup of drilling fluid brought on by the invasion of the wellbore by formation fluids and cuttings (Bageri et al., 2020). The rheological characteristics of drilling mud increase with the amount of clay present in the current formation being drilled (Bageri et al., 2020).

1.3 Rheological properties challenges in geothermal well drilling

The stability of drilling fluid for geothermal well application may be subdivided into chemical and physical, both are significant to achieve a successful drilling operation. The chemical stability of drilling mud may be referred to as the inhibitive resistance of the mud's chemical makeup to contamination, while physical stability is the ability to withstand the harsh HPHT, and high ROP inflicted on the mud by the downhole environment (Bageri et al., 2019).

The HPHT conditions present in the geologic location of the geothermal reservoir enhance the thermal degradation of polymeric components of drilling fluid. Therefore, maintaining the appropriate drilling fluid characteristics becomes very difficult at elevated temperatures (Avci and Mert, 2019). The common type of drilling fluids employed for drilling geothermal reservoirs is water-based mud (WBM) with bentonite as a viscosity-increasing additive, while other categories of additives such as fluid loss, pH, and rheology enhancers are also added for specific purposes.

Gelation, an important rheological property is mostly affected by the impact of elevated temperature of the geothermal reservoir. This was experienced and reported for geothermal drilling in the United States (Liles et al 1976; Tuttle and Listi 2003). The gel strength of drilling mud is the ability of the mud to develop a gel structure during the quiescent period and suspend drilled cuttings from falling to the bottom of the hole when circulation is ceased. Additionally, the aggradation of bentonite clay is another challenge of bentonite WBD at elevated temperatures.

Solid sag could also result from the drilling fluid's instability. The settling of weighting material like barite, ilmenite, and hematite due to their high specific gravity, from the mud column to the bottom of the hole is called sagging. This creates instability and varies the density in the fluid column. Solid material sagging may inflict operational threats such as variations in mud weight,

mud loss, and difficulties in well control (Bern et al., 2010; Zamora et al., 2004). The occurrence of kick is inevitable when the hydrostatic pressure is insufficient to prevent the flow of formation fluid into the wellbore. The bed formed by the settled solid material might pose drilling and completion challenges. The physical visualization of this is presented by Figure 3.

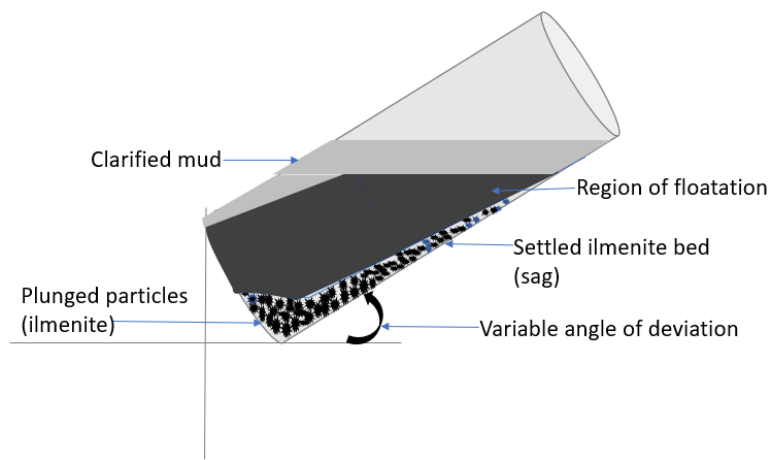


Figure 3. Schematic of an incline sag phenomenon (Oni et al., 2023).

As seen in Figure 4, the efficient transportation of drill cuttings from the wellbore to the surface is one of the basic functions of drilling fluid. For efficient hole cleaning to take place, there must be timely and adequate transportation of drill cuttings to the surface. Otherwise, it may lead to the deposition of cutting beds common in inclined wells when the inclination is between 45° - 75° (Oni et al., 2023), its deposition may be supported by angle of deviation, wellbore architecture, rheological characteristics, and mud's rate of flow. Busahmin et al (2017) identified other factors contributing to proper hole cleaning as the rate of penetration, cuttings texture, depth, and wellbore

geometry. Drilling mud's yield point demonstrates its capacity to suspend solid particles and drill cuttings (Fadairo et al., 2018). Hole cleaning is thought to be most difficult because of the high temperatures found in geothermal wells (Busahmin et al (2017) because it significantly alters the rheological characteristics of drilling fluid, and changes how the wellbores are being cleaned. In contrast, geothermal wells are drilled and completed with a greater hole size than HPHT oil and gas wells in order to increase fluid output and collect more energy. Therefore, the annular fluid velocity which is a primary determinant of cuttings transport is influenced by hole size in geothermal drilling (Naganawa and Okabe, 2014).

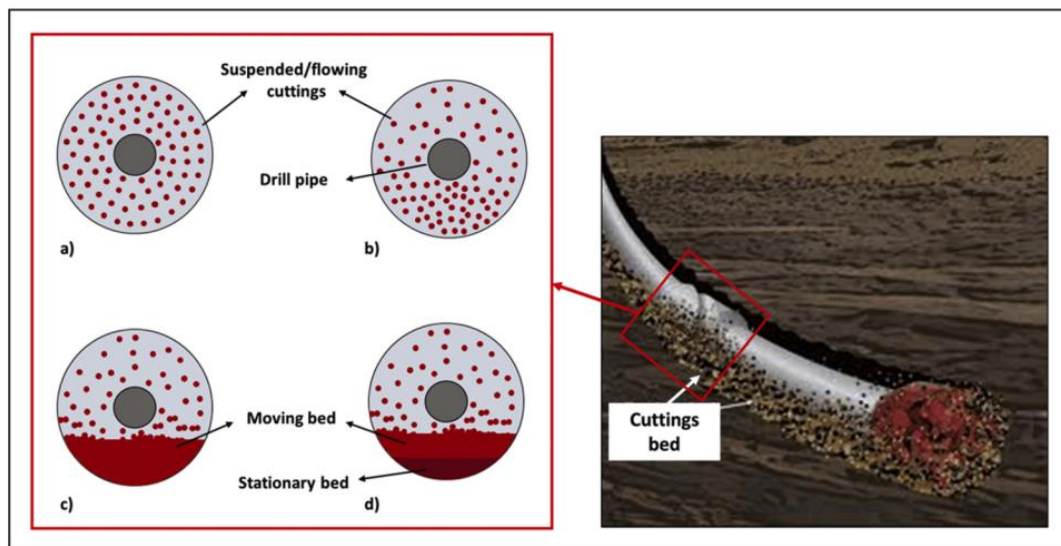


Figure 4. Deposition of drilled cuttings bed (Mahmoud et al., 2021).

1.4 A typical field challenge of sag phenomenon; Gulf of Mexico

The jeopardy of the sagging phenomenon was encountered while drilling a highly deviated well in the Gulf of Mexico at a deviated angle of 68. This threat occurred on three consecutive occasions

within this depth; 3183 – 4063 m MD; the first instance was after tripping out of the hole at 3,953.3 m to appraise the blowout preventer (BOP). Secondly, when the liner was being run. Thirdly, immediately after installing the production tubing. This sag-prone internal was drilled by utilizing a water-based mud of 12 ppg density, the drill bits penetration rate was within 9.1 – 12.2 m/hr. The rheological characteristics of the fluid are as follows; low shear yield point (LSYP) = 4- 6 lb./100 ft, Plastic viscosity (PV) = 18-21 Cp, yield point (YP) = 15 – 17 lb/100ft. The sagging was believed to be initiated by inadequate rheological characteristics, and low pipe rotation. To overcome the sagging challenge, the mud was treated with the addition of biopolymer and bentonite on each occasion (Mohamed et al., 2022). Therefore, a key factor in reducing the stability concerns with drilling fluid is choosing the optimum drilling mud formulation and maximizing its rheological qualities. The application of knowledge acquired in solving HPHT oil and gas wells can also be applied to geothermal well drilling due to close characteristics.

A geothermal well with a total depth of 3002 m (9850 ft) and an inclination of 70⁰ dug in Japan was investigated by Naganawa and Okabe (2014). The hydraulics and hole-cleaning capability of this extended reach well was evaluated. A combination of simulation and experimental approaches were deployed for this study. A flow loop test was conducted on the collected drilled cuttings, and the deviation started from vertical (0⁰) through horizontal (75⁰) while observing a 15⁰ increment in the angle of inclination. To have realistic optimization results, field-obtained data like equivalent circulation density (ECD), the type of mud, and mud flow rate were optimized for effective hole cleaning. The outcome of the study suggested it is paramount that wellbore hydraulics be included in the design phase of a geothermal drilling fluid for an effective drilling process.

CHAPTER II

LITERATURE REVIEW

2.0 Geothermal Wells in the United States

In 1976, 13 deep surveillance holes and 52 wells were sunk in the states of Utah, Oregon, Nevada, Idaho, and California to search for and develop geothermal resources. Eight are now halted, five were abandoned, and 39 (or 75% of the total) are now thought to have successfully discovered at least possibly commercial volumes of steam or hot water. Next to this, four significant production improvements were accomplished at The Geysers, along with the discovery of two additional fields in the Imperial Valley and Nevada (Smith et al., 1976). The first geothermal well in The Imperial Valley of California was created using clay mud.

2.1 Geothermal well drilling fluid systems.

Water has been employed as the continuous phase, and bentonitic clay as the dispersed phase in the design of water-based mud in the early stages of geothermal well drilling. To preserve and enhance the filtration and rheological characteristics of the drilling fluid, certain polymer additives are added (Zilch et al., 1991). Due to the cost and environmental friendliness of water-based mud over oil-based mud, it is the choice of most mud engineers. However, oil-based mud is more efficient in geothermal drilling because of its higher thermal stability. Additionally, the use of geothermal spring brine as a base fluid to create drilling mud for geothermal wells was tested. The earliest geothermal well located in The Imperial Valley in California was drilled with clay mud in 1976. The changes in rheological properties were recorded at 121⁰C, which discouraged the subsequent use of clay mud for geothermal well drilling (Zilch et al., 1991). As a result of this,

bentonite clay was replaced with sepiolite clay owing to its higher thermal resistance, to certain polymers were added to buffer it and enhance its filtration behavior (Tuttle, 2005). Copolymers were discovered and added to geothermal drilling mud design to increase its rheology and thermal stability. Currently, geothermal drilling fluid is now being designed with thermal resistance synthetic or natural polymeric additives. Bentonite is augmented with polymeric additives in other to reduce the cost. The use of nanoparticles in geothermal drilling fluid formulation was also investigated (Boyou et al., 2019). Above all, the thermal degradation of drilling fluids additives at HPHT and the cost of formulation have been a challenge militating against the drilling of more geothermal wells.

Drilling fluid performs several functions during drilling including maintaining borehole stability, carrying drilled cuttings to the surface, lubricating the drilling string, and preventing formation fluids from flowing into the wellbore (Adesina et al., 2012). The filtrate loss and the growth of filter cake around the wellbore during drilling operation affect the flow efficiency and raise the overall drilling expenses. It is impossible to overstate how crucial particle size distribution (PSD) of ultrafine calcium carbonate is to the filtrate loss process. It is therefore necessary to note that there is a direct relationship between PSD and filtrate loss. As such, the smaller the PSD, the smaller the volume of filtrate loss and vice-versa (Ezeakacha et al., 2017). The quality of the filter cake is physically and chemically influenced by the drilling fluid additives which include weighing and filtration agents. Barite is popularly utilized as a weighing substance in drilling mud formulation due to the number of benefits offered which include affordability, accessibility, and high specific gravity. However, a significant drilling operation usually demands a large amount of barite usage, hence causing mud cake thickness which can subsequently damage the formation and later impair the flow of reservoir fluids after the drilling operation (Fadairo et al., 2018; Li et al.,

2019). Besides, barite also exhibits a sagging problem which is the inability to suspend cuttings for a long period when drilling operation is not in circulation, thus further increasing formation damage and making it challenging to remove the filter cake from the walls of drilled wells (Elkatatny, 2019) even in the presence of acid. The right design of drilling fluid that engenders a thin, impervious filter cake is highly desirable to increase the efficiency of the drilling operations. Therefore, special attention is needed to effectively select an alternate weighting substance as a substitute for barite.

Due to the urgent need of the drilling industry to mitigate sagging, several materials such as copolymer, urea-based, organophilic clay, perlite, Nano silica, polyethylene glycol, diminution of densifying materials (barite, ilmenite, hematite, vermiculite), a combination of diminutized weight-materials have all been utilized in the drilling mud and investigated as anti-sagging agents to mitigate the occurrence (Al-Abdullatif et al., 2014; Al-bagoury, 2014). Al-bagoury (2014) explored the use of diminutized ilmenite as a weighing agent in both water-based and oil-based mud. Oni et al. (2023) suggested that even though sag occurs in both inclined and vertical wells, its effect is more threatening in inclined wells due to the variable angles of inclinations that may support a higher rate of settling out of fluid columns. They concluded that the severity of sagging is highest at 45° – 75° inclinations.

Ilmenite is an iron ore mineral (FeTiO_3), a titanium-iron oxide, with a steel-gray or weak magnetic solid, black in color, and trigonal crystal system. It has a specific gravity of $4.5\text{--}5.1 \text{ g/cm}^3$ which claimed advantages over barite due to its greater specific gravity, and its higher solubility in acid (Mohamed et al., 2019; Basfar et al., 2019). Therefore, compared to barite, less ilmenite intake is required to achieve the appropriate drill mud density, decreasing the solid ratio in mud.

Several filtration additives have been investigated to improve drilling fluid characteristics over the years. Environmental agencies have imposed tight regulations for drilling fluid additives because some of these compounds may have unfavorable effects on the environment (Al-Hameedi et al., 2019). Due to this, there is a trend in the oil and gas industry to use ecologically friendly drilling fluid additives to lessen their negative effects on the environment while also enhancing drilling fluid performance. A variety of cost-effective and eco-friendly natural materials which include clays, polymers, copolymers, and nanomaterials have been utilized to enhance the drilling fluid's qualities particularly low filtrate loss (Medhi et al., 2021). One of these is perlite (Bageri et al., 2020), which was combined with ilmenite, and suggested to be used as a filtration agent. It was proven that perlite greatly enhanced the filter cake's characteristics, with improvements in permeability and porosity of 23% and 31%, respectively. Perlite was discovered to have improved the rheological properties of the barite drilling fluid and eliminated the sagging problem (Mohamed et al., 2020). However, perlite is not readily available in North Dakota, unlike fly ash which is found to be abundant because is a by-product of lignite coal-fired plants.

In addition, fly ash is cost-friendly and cheaper than other inorganic ultrafine calcium carbonates that perform similar roles of plugging agents in water-based drilling fluid. For instance, ultrafine (0.02-0.36 μm) calcium carbonate cost like 305 to 610 €/ton, wollastonite 38 and 74 μm may cost 210 and 154 €/ton respectively, and precipitated calcium carbonate powder (not ultrafine) which may be cheapest goes for 120 €/ton (Teir et al., 2005). Conversely, the fly ash which is readily available, was obtained from the Antelope Valley power station, Mercier County, City of Beulah, North Dakota, United States. Fly ash is made up of tiny, powdery particles that are frequently spherical, hollow, or solid, and mostly glassy (amorphous) in composition. The angular particles make up the carbonaceous component in fly ash. Some of the physicochemical properties

of fly ash include specific gravity, which is between 1.6 and 2.6, a porosity of 30 to 65 %, pH ranging from 6 to 8, low free swell index, a surface area of about 5 m²/g, non-plasticity, lime reactivity of 1 to 8 MPa, bulk density of 900 to 1300 kg/m³, and extreme particle size of 0.001 to 0.1 mm (Gollakota et al., 2019). Fly ash's color can range from tan to gray to black, depending on how much of its carbon is unburned. The adsorption, particle size distribution, surface area, hydrophilicity, and porosity are important for water treatment (Mushtaq et al., 2019). The chemical and physical properties of fly ash make it useful material for a variety of applications like wastewater treatment, removal of organic solvents and inorganic pollutants, and removal of metals, boron, radioactive elements, and phosphates, in the construction industry, and in the production of geopolymers (Alterary and Maraei, 2021).

Fly ash can lessen the permeability of saturated, hardened cement pastes, as Marsh et al. demonstrated in 1985. The pozzolanic reaction of a class C fly ash to concrete caused a significant reduction in permeability (Afroz et al., 2023; Guarav et al., 2023). According to these studies, fly ash as a binder is ideal for replacing a portion of cement in concrete (up to 25%) without negatively impacting the strength. To fully comprehend the potential and constraints of fly ash, more study into its utilization in various drilling fluid formulations is still needed.

CHAPTER III

METHODS

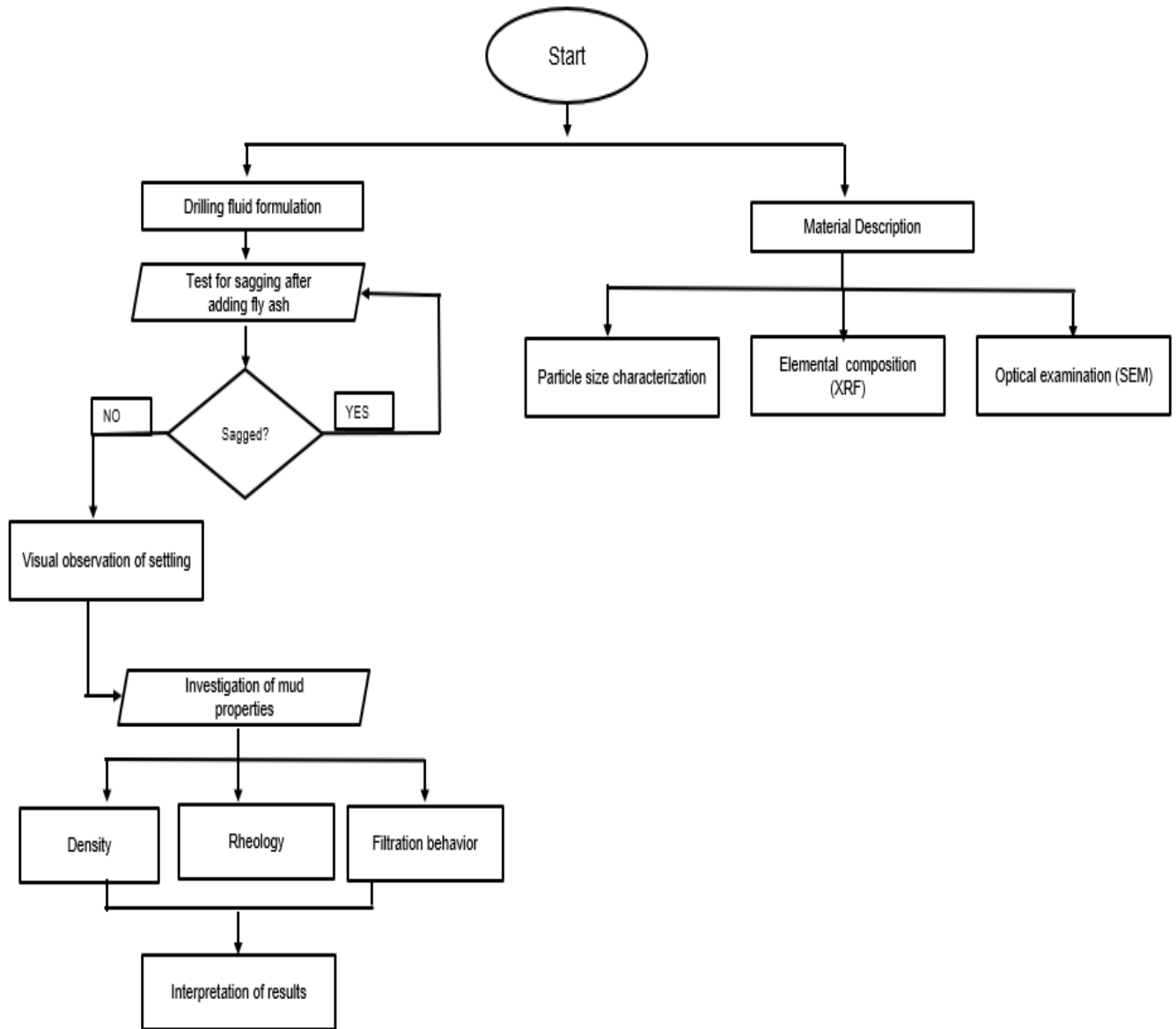
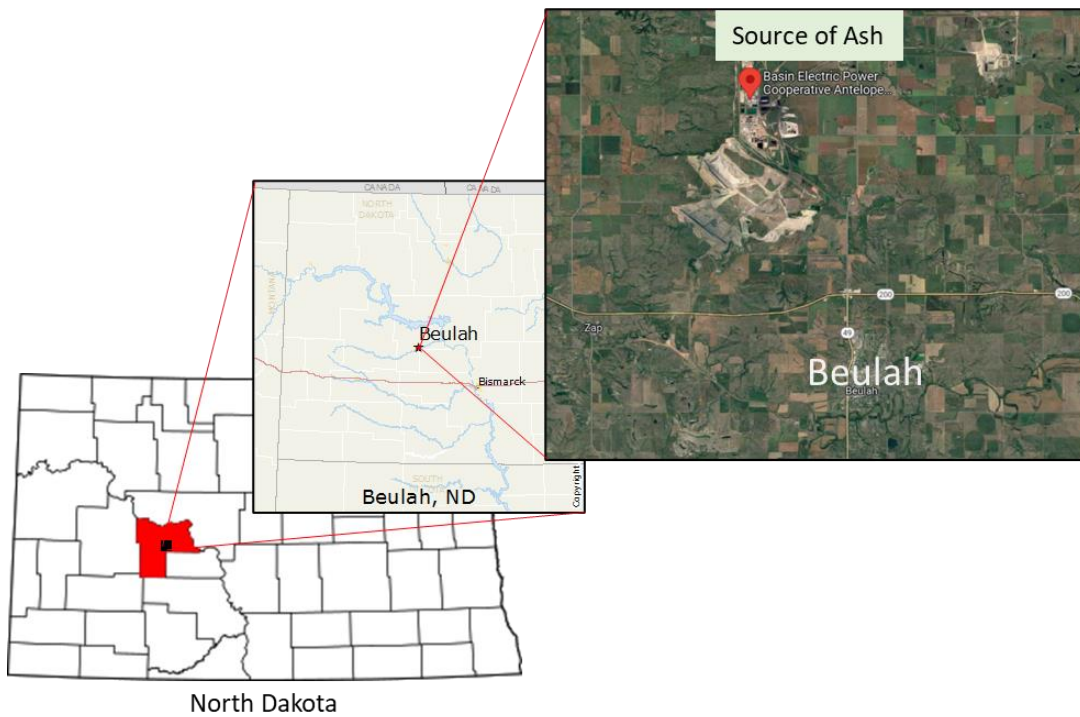


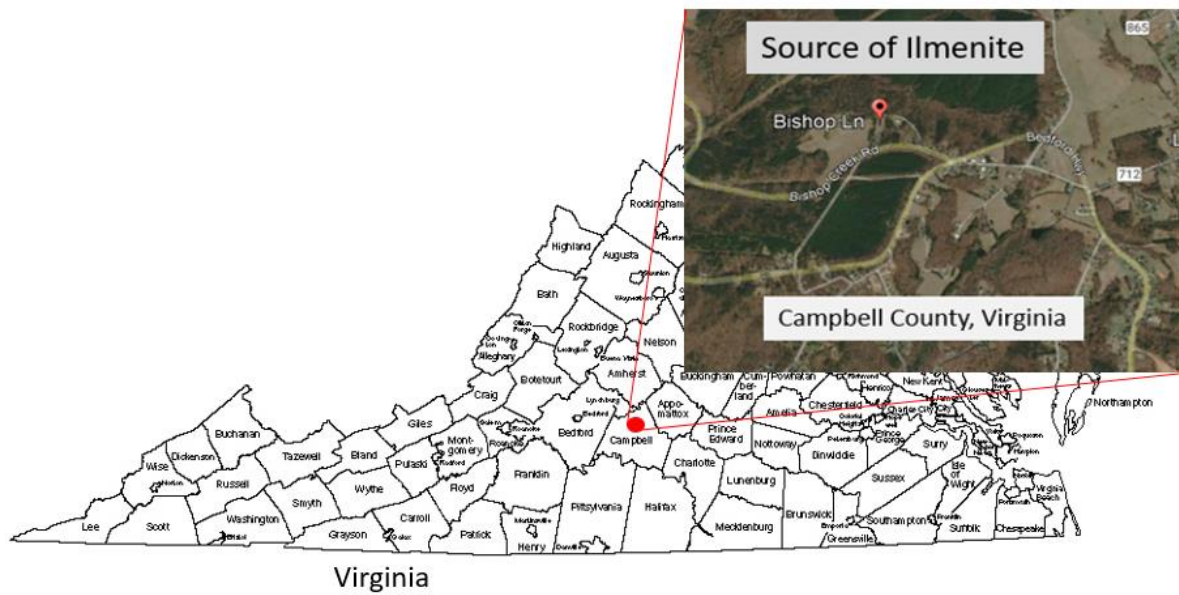
Figure 5. Experimental flowchart

3.0 Materials

The fly ash and ilmenite used in the study were respectively obtained at Antelope Valley power station, Beulah, North Dakota, and Bishop Mine, Campbell County, Virginia, United States. Figure 6 further describes these locations. Industrial copolymer, Bentonite, and Calcium Carbonate were sourced from Newpark Resources an oil and gas drilling fluids company in the United States while other chemicals were procured from the chemical market in the states.



(a)



(b)

Figure 6. Locations where fly ash and ilmenite samples were collected respectively: (a) Fly ash obtained from Antelope Valley power station, Mercer County, City of Beulah, North Dakota, and (b) Bishop Mine, Campbell County, Virginia, United States.



Figure 7. Stack of sieves with fly ash sample.



Figure 8. Stack of sieves with fly ash sample placed in a sieve shaker.

Figures 7 and 8 show the pictorial illustration of the sieves and sieve shaker machine utilized in the determination of PSD. For fly ash and ilmenite, the PSD data showed aggradation (D50) of 130 and 62 μm , respectively. Utilizing a scanning electron microscope (SEM), optical examination of particle surfaces revealed that the spherical shape of fly ash particles varies in size and shape gradation, in contrast with the irregular, sub-rounded, or rounded shape of ilmenite that has smaller particles, as shown in Figure 10 (Bageri et al., 2022). The SEM micrograph of ilmenite and fly ash were depicted in Figures 10 and 11 respectively.

D50 of the sieve analysis results were carried out on both ilmenite and fly ash to assess the influence of relative particles on the volume of filtrate in the formation during the drilling operation. Figure 9 shows that the particle size distribution for both ilmenite and fly ash is 62 μm and 130 μm respectively as demonstrated in the particle sieve analysis of D50. The scanning electron microscopy (SEM) of pure ilmenite and pure fly ash particles has been previously reported by some authors (Bageri et al., 2022) and (Singh et al., 2023) respectively as displayed in Figure 10 and Figure 11. Fly ash particles have a spherical shape, which increases their ability to seal the gaps between the particles in the mud cake, while ilmenite particles could be irregular, angular, or rounded in shape, according to SEM pictures (Bageri et al., 2022). The shape of pure ilmenite particles was suggested to vary from angular to rounded (Jabit et al., 2018). X-ray diffraction analysis was conducted in this study to determine the chemical composition in weight percent of Beulah lignite fly ash as reported in Table 1. The chemical composition of pure ilmenite and pure fly ash was determined by energy dispersive X-ray analysis (EDS), as shown in Figure 10 and Table 1. Figure 12 further expresses the representation of chemical composition in weight percent of Beulah lignite fly ash as revealed by X-ray diffraction analysis. The main elements of pure

ilmenite were depicted in Fig. 3 in the following proportions: titanium (Ti), oxygen (O), and iron (Fe), with 35.7 wt%, 33.7 wt%, and 27.6 wt%, respectively. Calcium (Ca), silicon (Si), and magnesium make up the final 3% (Mg). As regards fly ash, the dominant compound is silicon oxide (SiO₂) with 24.5398 wt%, Calcium oxide (CaO) with 17.744 wt%, sodium oxide (Na₂O) with 15.8441 wt%, iron (III) oxide (Fe₂O₃) with 11.2066 wt%, aluminum oxide (Al₂O₃) with 10.9579 wt%, sulfur trioxide (SO₃) with 10.677 wt%, magnesium oxide (MgO) with 5.1362 wt %, and potassium oxide (K₂O) with 1.9415 wt% as also seen in Table 1. The minor compounds present include strontium oxide (SrO), phosphorus pentoxide (P₂O₅), barium oxide (BaO), titanium dioxide (TiO₂), and zirconium dioxide (ZrO₂) which represents 1.9529 wt%.

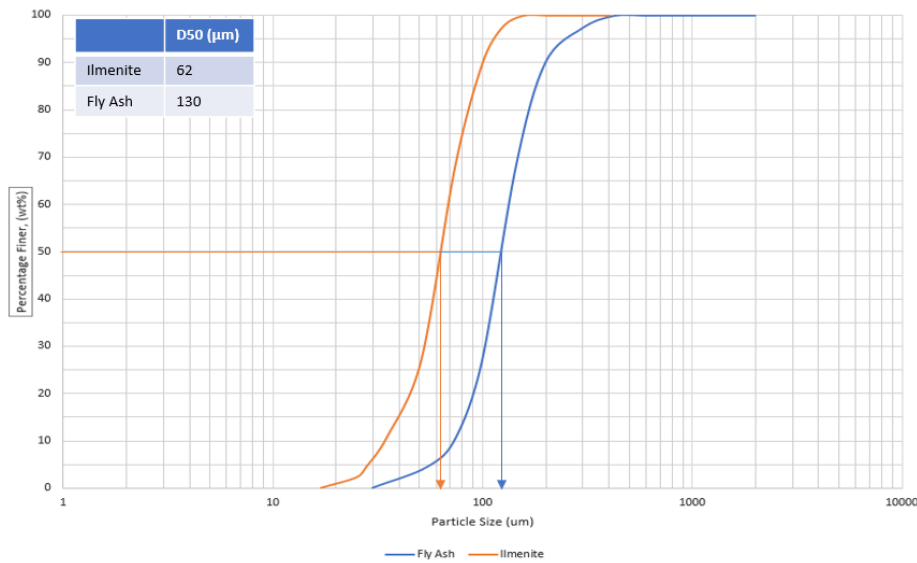


Figure 9. The Particle size distribution (D50) for ilmenite and fly ash.

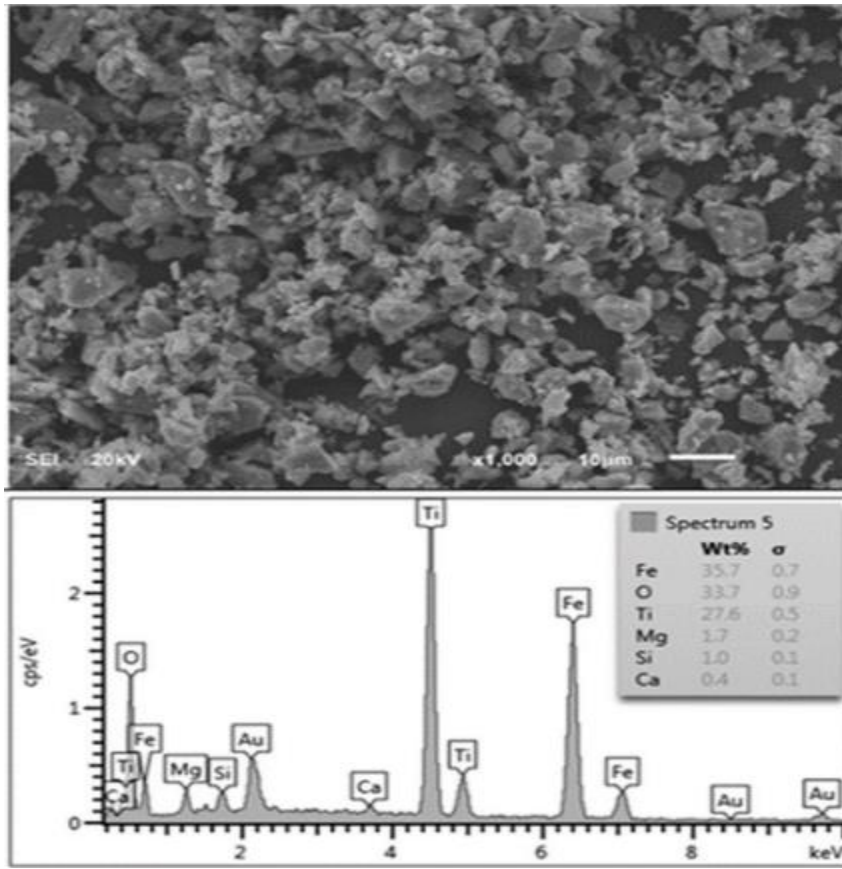


Figure 10. SEM (high-resolution) imaging was performed on the ilmenite densifying additive (Bageri et al., 2022).

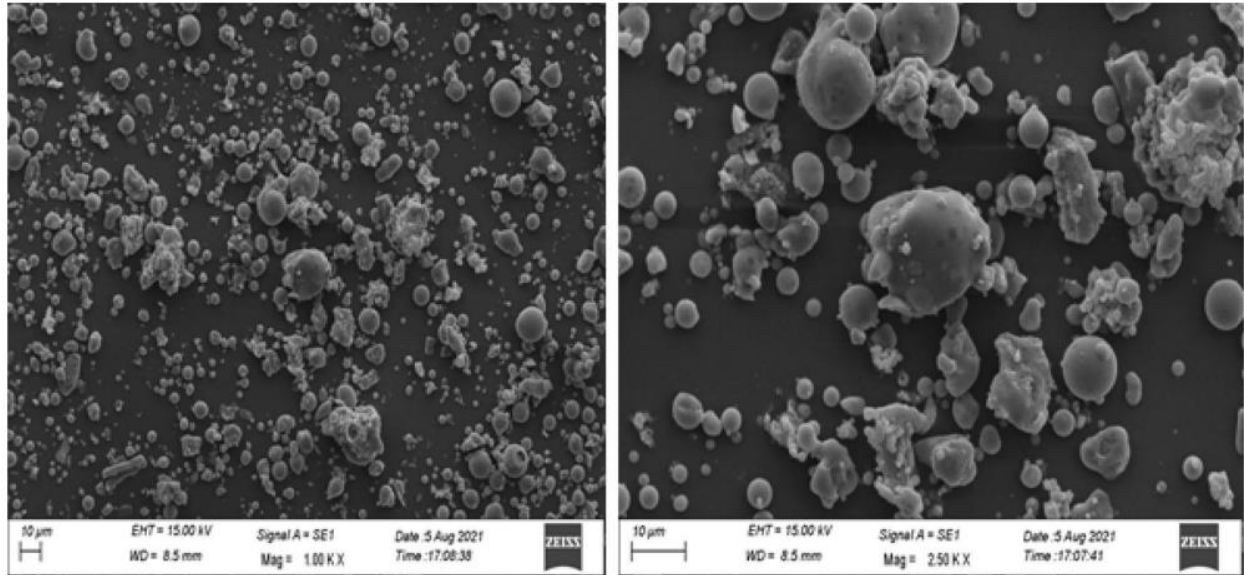


Figure 11. SEM micrograph of fly ash (Singh et al., 2023).

Table 1

Analysis Beulah Lignite fly ash.

Component	Result (mass%)
SiO ₂	24.5398
CaO	17.744
Na ₂ O	15.8441
Fe ₂ O ₃	11.2066
Al ₂ O ₃	10.9579
SO ₃	10.677

MgO	5.1362
K ₂ O	1.9415

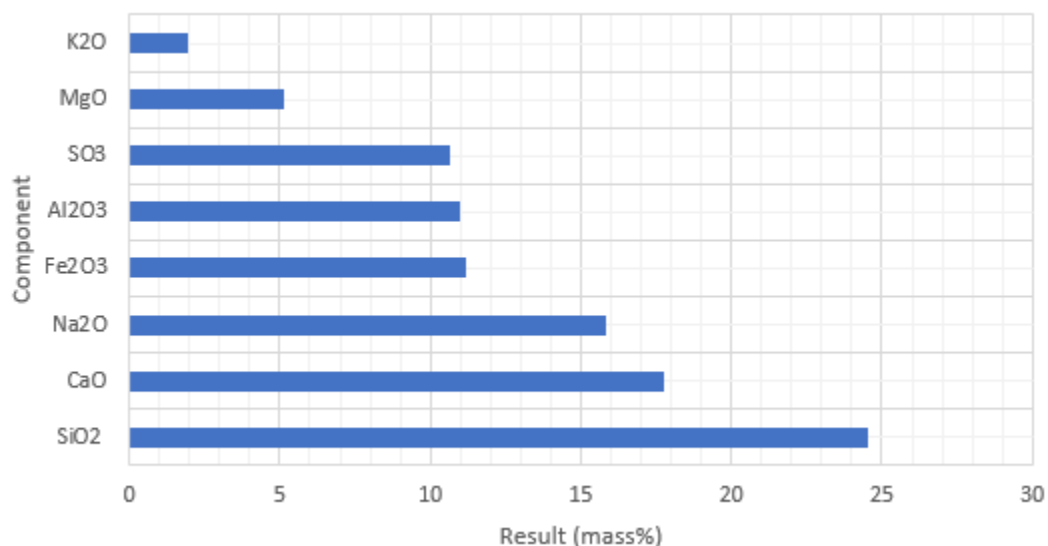


Figure 12. X-ray diffraction analysis of Beulah Lignite fly ash.

3.1 Drilling fluid sample preparation

350 cm³ of WBM were prepared using a Hamilton Beach multimixer at ambient temperature. Table 2 provides a description of the mud formulation along with the applied concentrations and functions. The base fluid was deionized water with the addition of supplementary materials sometimes called additives. The additives are among the ones that are most frequently utilized in oil and gas drilling applications, they were chosen since they were readily available and relatively inexpensive. Different amounts of the proposed fly ash were added to the Base Mud (0, 1, 2, and 3 lb./bbl) as a sag-resisting material. As a weighing agent, ilmenite (FeTiO₃) particles were introduced at a consistent quantity (350 lb./bbl).

Table 2.

Composition of a drilling fluid barrel

	Function	Unit	Base Mud	Base Mud + 1 lb/bbl of fly ash	Base Mud + 2 lb/bbl of fly ash	Base Mud + 3 lb/bbl of fly ash
Water	Continuous phase	Bbl	0.7	0.7	0.7	0.7
Potassium Hydroxide	Alkalinity control	Lb	0.5	0.5	0.5	0.5
Fly ash	Sag control agent	Lb	0	1	2	3
Calcium carbonate	Bridging material	Lb	5	5	5	5
Defoamer	Anti-foam agent	Lb	0.08	0.08	0.08	0.08
Industrial Copolymer	Copolymer	Lb	1	1	1	1
PAC-R	Polymer	Lb	1	1	1	1
Xanthan gum	Viscosity control	Lb	0.5	0.5	0.5	0.5
Ilmenite	Weighting agent	Lb	350	350	350	350
Corn starch	Fluid loss control	Lb	6	6	6	6

Soda ash	Maintains calcium level	Lb	0.5	0.5	0.5	0.5
Bentonite	Viscosity control	Lb	4	4	4	4
Potassium chloride	Shale stabilizer	Lb	20	20	20	20

The industrial copolymer was added to the mud samples to raise thermal stability and improve rheology. Newpark Resources provided the novel copolymer, and it is made up of partially hydrolyzed polyacrylamide (PHPA) as a functional additive with a 3% solution, and an acidity level of 9.10. The novel copolymer easily disperses in water without forming fisheyes. This copolymer's primary uses are as a flow improver, as well as clay and shale inhibitor.

Fly ash particles have a spherical shape, which increases their ability to seal the mud cake's voids between its pieces, while ilmenite particles could be irregular, angular, or rounded in shape, according to SEM pictures (Bageri et al., 2022).



Figure 13. A multimixer machine with cups.

3.2 Drilling fluid properties measurement

Sag test

To evaluate the fly ash's effectiveness as an anti-sagging agent, statically and dynamically positioned sagging studies were executed. The stable test was conducted on Base Mud (0 lb./bbl of fly ash) and Base Mud plus 3 lb./bbl of fly ash over a range of temperatures (250⁰F, 300⁰F, 350⁰F, and 400⁰F) at different angles of inclination (30⁰, 45⁰, 60⁰, 70⁰, 80⁰ and 90⁰) while observing API standard procedure. The HPHT Ofite Filter Press was redesigned with the addition of an inclination meter for this purpose as displayed in Figure 14a. A volume of 140 cm³ of drilling mud was emptied into the cell cup with the exclusion of the metal stand (Figure 14b). After that, it was inserted into the redesigned filter press (Figure 14a). To prevent fluid from vaporizing, a 500-psi pressure of nitrogen gas was applied. After the sample had been aged for 24 hours at various

temperatures and inclinations, a volume of 10 cm³ of the sample was sucked from the top of the cell through the cannula into a calibrated syringe. The mass was obtained and divided by volume to have a density at the top. Similarly, the same process was repeated but sucked from the lowermost part of the cell, and the following equations were applied to the obtained results:

$$\rho_{bottom} = \frac{\text{Mass of sample obtained at the bottom}}{\text{Volume of sample obtained at the bottom}} \quad (1)$$

$$\rho_{top} = \frac{\text{Mass of sample drawn from the top}}{\text{Volume of sample drawn from the top}} \quad (2)$$

$$\text{Sag Factor (SF)} = \frac{\rho_{bottom}}{\rho_{bottom} + \rho_{top}} \quad (3)$$

ρ_{bottom} = Density of mud at the bottom of the cup

ρ_{top} = Density of mud at the top of the cup

The sag factor (SF) illustrates the susceptibility of the weight-material to either free or hindered settling. A high SF number indicates a stronger tendency to sag. The safe zone for sag factor is between 0.5 and 0.53, which is the permissible range (Alabdullatif et al., 2014). Additionally, the well geometry significantly influences the sagging factor. To simulate deviated wells, the redesigned HPHT was used, and the same test was run at various inclinations (i.e., 30⁰, 45⁰, 60⁰, 70⁰, 80⁰, and 90⁰).

Additionally, the VSST, as depicted in Figure 14c, was used to conduct the dynamic sagging test. For this analysis, a speed of 100 revolutions per minute and a temperature of 120⁰F was applied to

140 cm³ of homogeneous sample in the thermo-cup for a duration of 30 mins. A volume of 10cm³ of the sample was sucked through the cannula into a calibrated syringe from the groove of the sag shoe inside the thermo-cup before and after spinning and recorded as weight before and after accordingly. The dynamic sagging propensity was calculated as follows using the test data:

$$VSST = 0.833 \times (W_{\text{after}} - W_{\text{before}}) \quad (4)$$

W_{after} = Weight of mud in the syringe after 30 minutes of stirring

W_{before} = Weight of mud in the syringe before stirring

The VSST measured in pounce per gallon (ppg) is an indication of the stability of the drilling mud, values below 1ppg represent stable (homogeneous mixture) mud devoid of sagging while values above 1.6 ppg are unstable (inhomogeneous mixture) mud, which may be the onset of sagging (Aldea et al., 2001; Mohammed et al., 2020). The region in between stable (1 and 1.6 ppg) may be referred to as the transition region or boundary between the stable and unstable sample.



(a)



(b)

Figure 14. Equipment for performing statically positioned sag tests: (a) oblique (30° , 45° , 60° , 70° , 80° , and 90°) and (b) vertical.

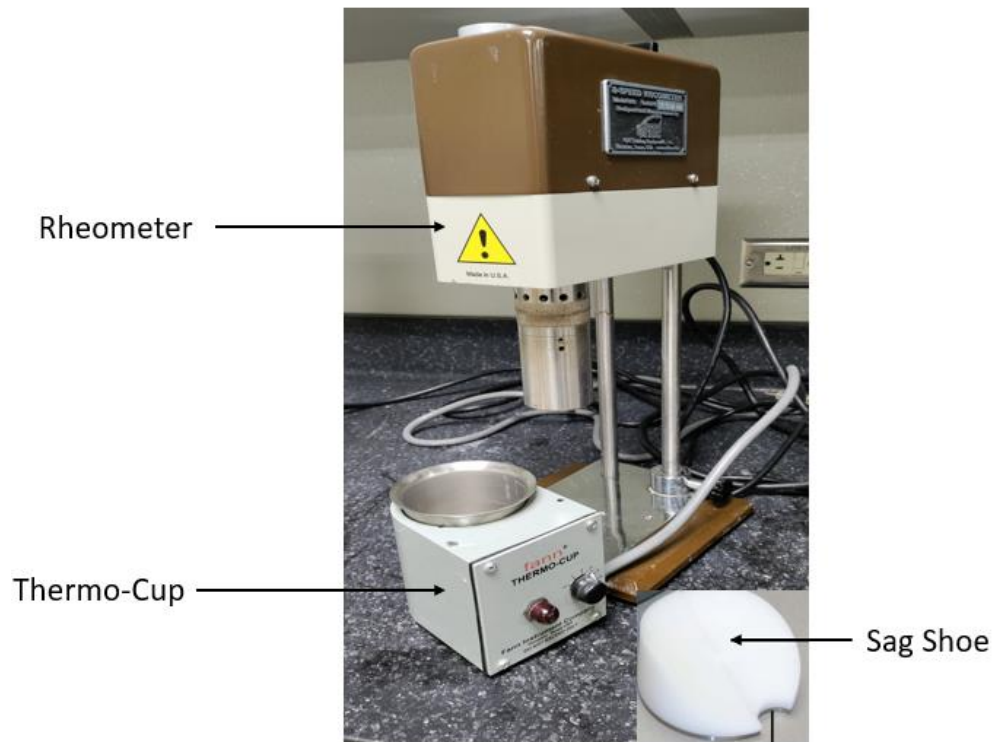


Figure 14c. VSST test major apparatus (syringe not included).

Mud density

The mud density was measured with the use of a four-scale mud balance. The apparatus was calibrated with distilled water to ensure accuracy. Subsequently, the density of the mud samples was determined and recorded in lb./gal (ppg).



Figure 15. A Mud balance.

Rheology

Using an OFITE viscometer (8-speed viscometer), the flow characteristics such as 10 mins and secs gel, plastic and apparent viscosity, and yield point were examined for the mud with various fly ash ratios of 0, 1, 2, and 3 lb./bbl were included in the Base Mud. Figure 16 shows the equipment used for this purpose. These tests were investigated at an elevated temperature (450⁰F).

The viscometer was turned to 300 and 600 revolutions per minute, and the values were recorded accordingly. The influence of the fly ash addition on the flow parameters, such as apparent viscosity, plastic viscosity, yield point, and gel strengths (10-s and 10-min), were investigated, and calculated using the formulae below:

$$\text{Apparent Viscosity (AV)} = \frac{\tau}{\dot{\gamma}}$$

$$\text{Plastic Viscosity (PV)} = \tau_{600} - \tau_{300}$$

$$\text{Yield Point (YP)} = \tau_{300} - PV$$



Figure 16. 8-Speed viscometer for measuring rheological properties.

Filtration behavior

Static filtration tests were conducted at 450⁰F (232⁰C) and 300 psi. The experiments were conducted on each of the mud samples listed in Table 2. The tests were performed on Base Mud plus 1, 2, and 3 lb./bbl of fly ash in the same manner, to further investigate the effect of fly ash on filtration characteristics. The filtration volume was determined during the fluid loss test as a function of time until the test's conclusion (30 min). Figure 17 shows the HPHT filter press equipment used to achieve this.



Figure 17. HPHT filter press with a measuring cylinder for collecting filtrate loss.

CHAPTER IV

RESULTS AND ANALYSIS

4.0 Sagging efficiency

In order to appraise how well the ilmenite drilling fluid performs both statically and dynamically when using fly ash, two samples were investigated for this purpose (Base Mud plus 0 lb./bbl of fly ash, and Base Mud plus 3 lb./bbl of fly ash), over several ranges of temperatures and angles of inclination. As depicted by Figure 18 and Table 3, Base Mud plus 0 lb./bbl of fly ash at 0° inclinations, and 250°F has the lowest sag factor of 0.504, followed by 300°F, 350°F, and 400°F with SF of 0.515, 0.521, and 0.527 accordingly. As observed from this figure, all the sagging tests investigated from 0° to 30° inclinations (250°F, 300°F, 350°F, and 400°F) were within the API-recommended sag factor region of 0.53 for static conditions though 250°F was the most stable. This may be due to the effectiveness of the atomic bonds of industrial copolymer at 250°F, it is worth noting that other polymers which are also Base Mud plus 0 lb./bbl of fly ash additives such as PAC-R, Corn starch, and xanthan gum typically degrade at or close to 250°F. An increment of 58% (0.516 to 0.519) of sag factor occurred within 250°F and 300°F over a temperature rise of 50°F. At 350°F, and 400°F were 96% and 38% sag factor increments respectively. The highest sag factor increments of 96% were observed to have taken place within 300°F to 350°F, over a rise of 50°F. Furthermore, it can also be deduced that Base Mud plus 0 lb./bbl of fly ash experienced the highest sag at angle 61°, in which the most noticeable sag occurs at 400°F (0.545), next to it are 350°F, 300°F, and 250°F at 0.542, 0.539, and 0.536 respectively. Generally, from the trend, the sag factor can be said to be increasing linearly at various temperatures (250°F, 300°F, 350°F, and 400°F) from 30° to 61°. After which, it begins to decrease linearly, and stops the steady decrease at 80°. The sag factor is equal at 80° and 90° for most temperatures except for 400°F which is 0.534 at 80°

and 0.533 at 90°. Looking at the response of the Base Mud plus 0 lb./bbl of fly ash additives to sagging, inclination, and thermal stability, from the trend, it may be said to have different resistance to sag, and deviation, at different temperatures. This may be the effect of heat on the copolymer, thereby making it to be less stable and inefficient to prevent the settling of mud components at the respective temperatures. At various temperatures of 250°F, 300°F, 350°F, and 400°F, sagging occurs at 40°, 44°, 49°, and 55° respectively, and beyond.

In comparison, as showcased by Figure 19, the outcome of the SF of the Base Mud plus 0 lb./bbl of fly ash performed under statically controlled conditions of 0° (straight-up) and (45°) oblique positions, resulted in 0.504 and 0.521 at 250°F. The influence of a steady increase in temperature from 250°F to 400°F increased the SF from 0.504 to 0.527 for the straight-up hole while that of 45° hole was raised from 0.521 to 0.532. At 45°, the effect of temperature on Mud 0 was prominent from 350°F to 400°F. This may be the resultant influence of an increase in the angle of deviation (0° to 45°) and temperature on the thermal stability of Mud 0 (0 lb./bbl of fly ash). In addition, a raise in the angle of deviation causes an increment in the surface area of the hole which encourages free settling of weight-material. Thus, sagging was initiated, and as may be observed there was a fast-sagging propensity at inclined than at vertical.

In summary, it can be inferred from Figure 19, that the higher the temperature the lesser the strength of the industrial copolymer's atomic bond to keep the ilmenite particle size of 62 µm in suspension, and the lesser the thermal stability of the Base Mud plus 0 lb./bbl of fly ash. Practically, it is predictable for a drilling crew to utilize this formulation to avoid drilling at these angles of inclinations; 40°, 44°, 49°, and 55° at 250°F, 300°F, 350°F, and 400°F respectively because of sagging tendencies.

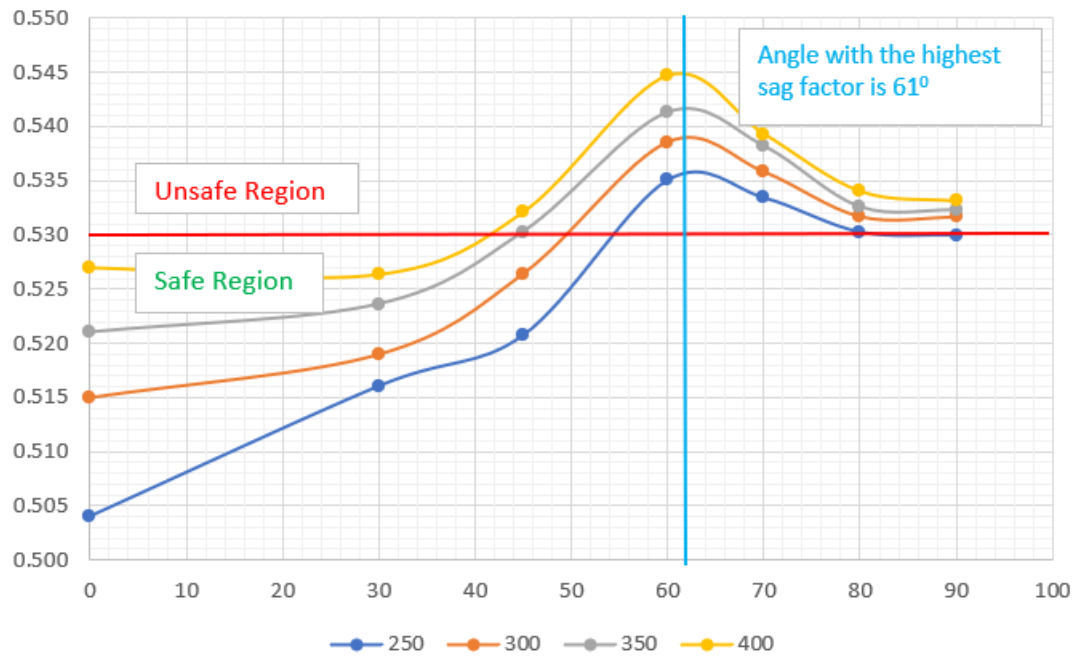


Figure 18. Static sag test for Base Mud plus 0 lb./bbl of fly ash at different angles of inclination and temperature.

Table 3.

Data of static sag test for Base Mud plus 0 lb./bbl of fly ash at different angles of inclination and temperature.

	250 ⁰ F	300 ⁰ F	350 ⁰ F	400 ⁰ F
0 ⁰	0.504	0.515	0.521	0.527
30 ⁰	0.516	0.519	0.524	0.526
45 ⁰	0.521	0.526	0.530	0.532
60 ⁰	0.535	0.539	0.541	0.545

70 ⁰	0.533	0.536	0.538	0.539
80 ⁰	0.530	0.532	0.533	0.534
90 ⁰	0.530	0.532	0.532	0.533

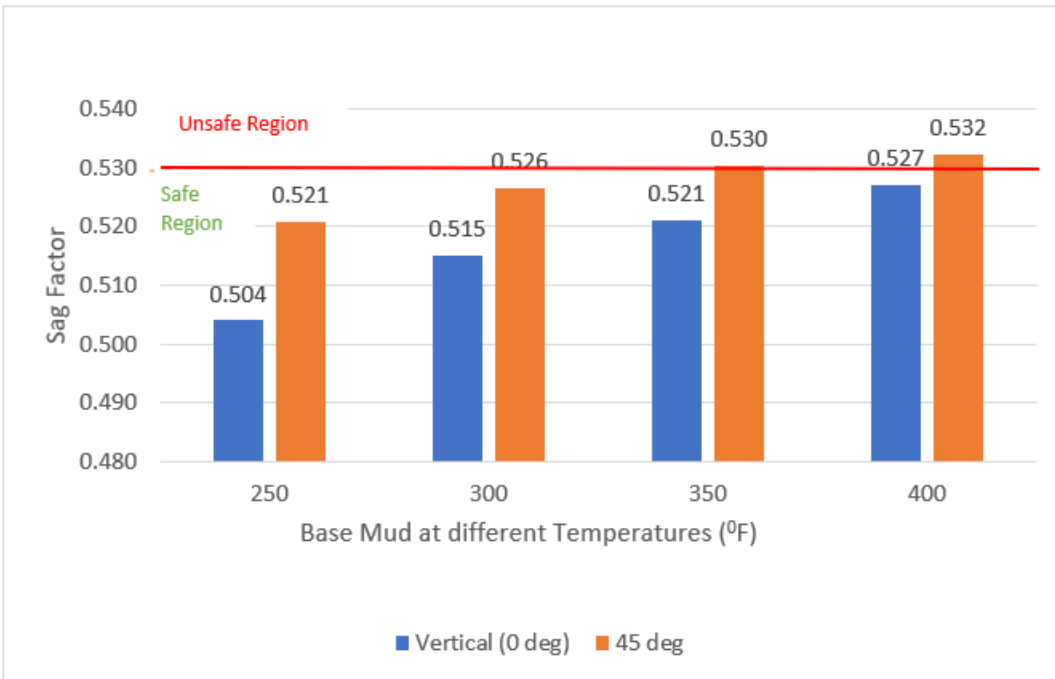


Figure 19. Static sag test for Base Mud (0 lb./bbl of fly ash) measured at 0⁰ and 45⁰ under different temperatures.

As can be seen from Figure 20 and Table 4, Base Mud plus 3 lb./bbl of fly ash experienced the highest sag factor at 60⁰ for all temperatures. However, 400⁰F has the highest sag factor of 0.528, other temperatures such as 350⁰F, 300⁰F, and 250⁰F have sag factors of 0.527, 0.525, and 0.520 respectively. At 250⁰F, Base Mud plus 3 lb./bbl of fly ash has a linear increase in sag factor from

0.508 (0°) through 0.520 (60°), this was succeeded by a linear reduction through 0.515 (90°). The 3 lb./bbl of fly ash added to this sample was efficient to prevent the sample from sagging (safe region) irrespective of the temperature and hole inclination investigated. The hole inclination at 60° under 300°F yielded the highest percentage increase in sag factor over a 50°F increment in temperature (250°F to 300°F). This may be due to the influence of heat on some polymeric additives in the mud sample. A polymer's onset of degradation may start around 300°F, and when this happens the mud loses its gel structures to some extent. Consequently, the suspension of weight material (ilmenite) is reduced, and ilmenite settles out of the static fluid column. Despite the effect of temperature and steady increase in hole deviation which supports sagging, fly ash of 3 lb./bbl was efficient to keep Mud Base plus 3 lb./bbl of fly ash sample stable, and within the API recommended standard value (safe region).

Comparatively, Figure 21 shows the static sag test for Base Mud plus 3 lb./bbl of fly ash as measured at 0° (vertical), 45°, and 60° under different temperatures of 250°F, 300°F, 350°F, and 400°F. From the literature, the hole with a 45° deviance has the highest sag factor (Ahmed et al., 2022; Basfar et al., 2022; Mohamed et al., 2020) while for this study 60° deviance presented the highest SF. Additionally, temperature and SF exhibited a directly proportional relationship. This result further supports the notable significance of hole deviation and temperature on solid sagging. As investigated, under the same temperature, but different inclinations the effect of hole deviation was further proven.

Practically, this mud formulation may be safe to utilize, if adopted to drill deviated well whose angle and reservoir temperatures fall within the scope of this investigation.

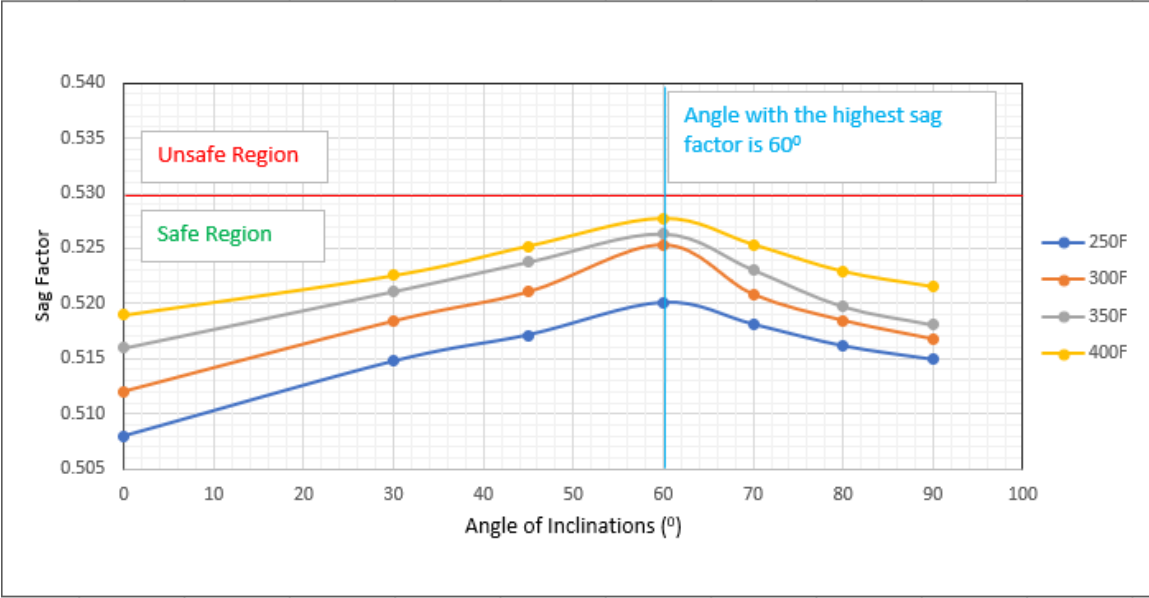


Figure 20. Static sag test for Base Mud plus 3 lb./bbl of fly ash at different angles of inclinations and temperatures.

Table 4.

Data of static sag test for Base Mud plus 3 lb./bbl of fly ash at different angles of inclination and temperatures.

	250 ⁰ F	300 ⁰ F	350 ⁰ F	400 ⁰ F
0 ⁰	0.508	0.512	0.516	0.519
30 ⁰	0.515	0.518	0.521	0.523
45 ⁰	0.517	0.521	0.524	0.525
60 ⁰	0.520	0.525	0.526	0.528
70 ⁰	0.518	0.521	0.523	0.525
80 ⁰	0.516	0.519	0.520	0.523

90 ⁰	0.515	0.517	0.518	0.522
-----------------	-------	-------	-------	-------

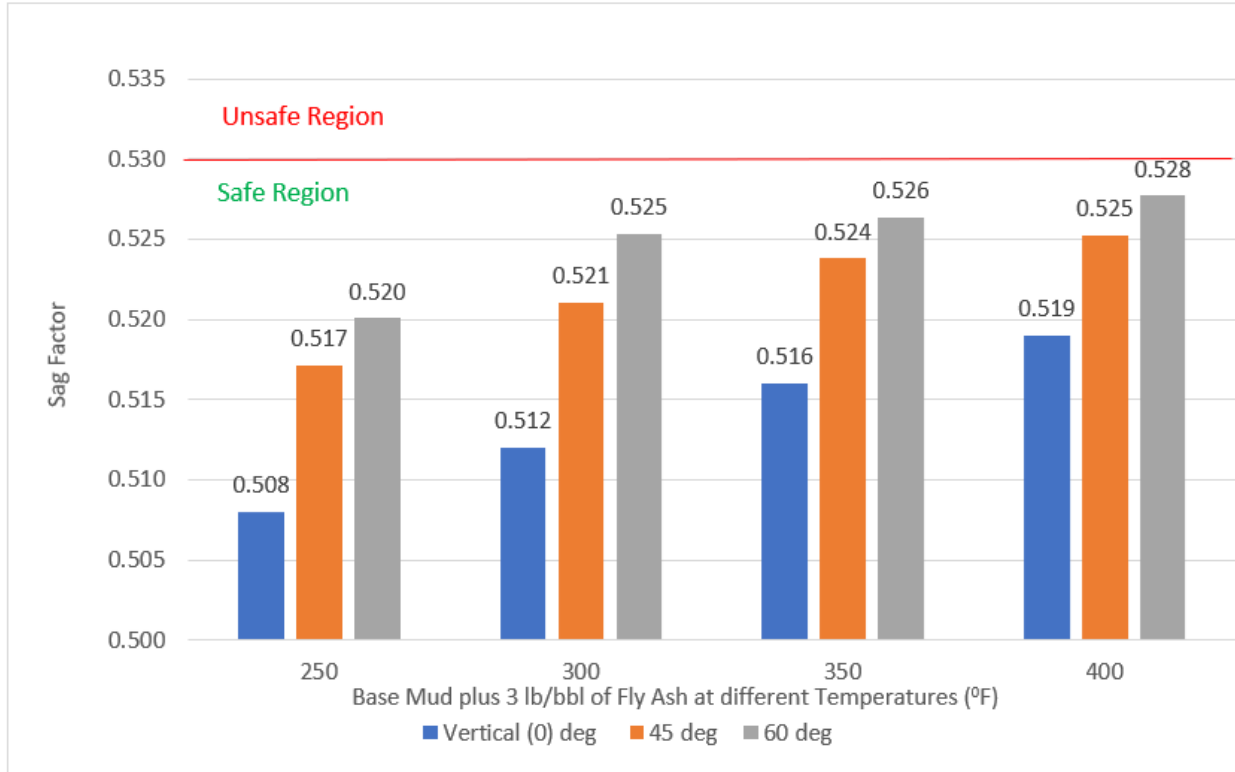


Figure 21. Static sag test for Base Mud plus 3 lb./bbl of fly ash measured at 0⁰ (vertical), 45⁰, and 60⁰ under different temperatures.

The dynamic conditions for the drilling samples Base Mud plus 0 and 3 lb./bbl of fly ash are shown in Figure 22. The Base Mud plus 0 lb./bbl of fly ash exhibited a high sagging propensity with an SF of 1.65, 1.7, 1.73, and 1.79 ppg at 250⁰F, 300⁰F, 350⁰F, and 400⁰F respectively. During the investigation, the highest percentage increase in sag factor was observed at 1.79 ppg (3.47%) over

a 50⁰F increment in temperature (350⁰F to 400⁰F), next to this was 1.70 ppg (3.03%), and the least was 1.73 ppg (1.76%). The unequal response of Base Mud plus 0 lb./bbl of fly ash mud sample to equal interval of temperature rise (50⁰F) may be due to the prominence of heat on the polymers and industrial copolymer. Xanthan gum and Corn starch are both polymer additives, while Industrial copolymer is a copolymer additive. These polymers degrade at different temperatures, and when this happens the mud loses its gelatinization and becomes watery. The sagging may be due to the inability of these polymers to withstand heat at 250⁰F and beyond.

Conversely, Base Mud plus 3 lb./bbl of fly ash demonstrated very stable tendencies which varied from 0.51, 0.52, 0.53, and 0.68 ppg at 250⁰F, 300⁰F, 350⁰F, and 400⁰F respectively. A percentage increase of 1.96%, 1.92%, and 28% was observed at 0.52, 0.53, and 0.68 ppg accordingly. Despite the biggest percentage increase in sag factor (28%) that occurred at 400⁰F, all the results of the investigated sag factor, at different temperatures still fell below the API recommended value of 1 ppg. However, it was obvious that an increase in temperature reduces the sagging stability. The 28% increase in sag factor at 400⁰F may be due to the fact that most polymer additive utilized may have attained their onset of thermal degradation before 400⁰F.

Comparatively, in the material formulation of Base Mud plus (0 and 3) lb./bbl of fly ash, the difference is the presence of 3 lb./bbl of fly ash. The influence of 3 lb./bbl of fly ash on the Base Mud sample may be said to be responsible for increasing the sagging stability of this sample. Fly ash is hydrophilic (about 2% dissolves in water) and polar in nature, this polarity enables it to form ionic groups. Its good suspending properties may be due to the polarity as well as additional characteristics like surface area, specific gravity, and pH (Mushtaq et al., 2019; Singh et al., 2022).

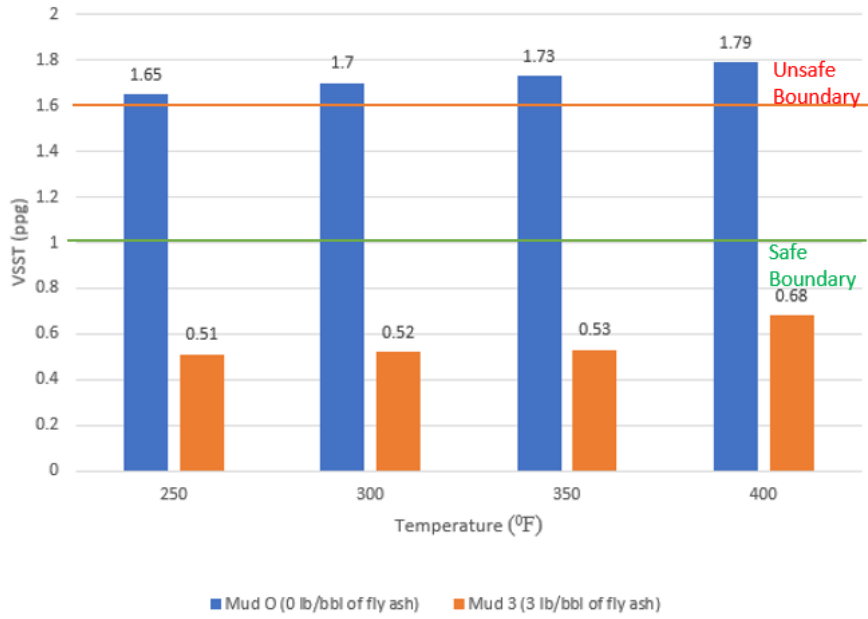


Figure 22. Dynamic sag test for Base Mud plus 0 and 3 lb./bbl of fly ash.

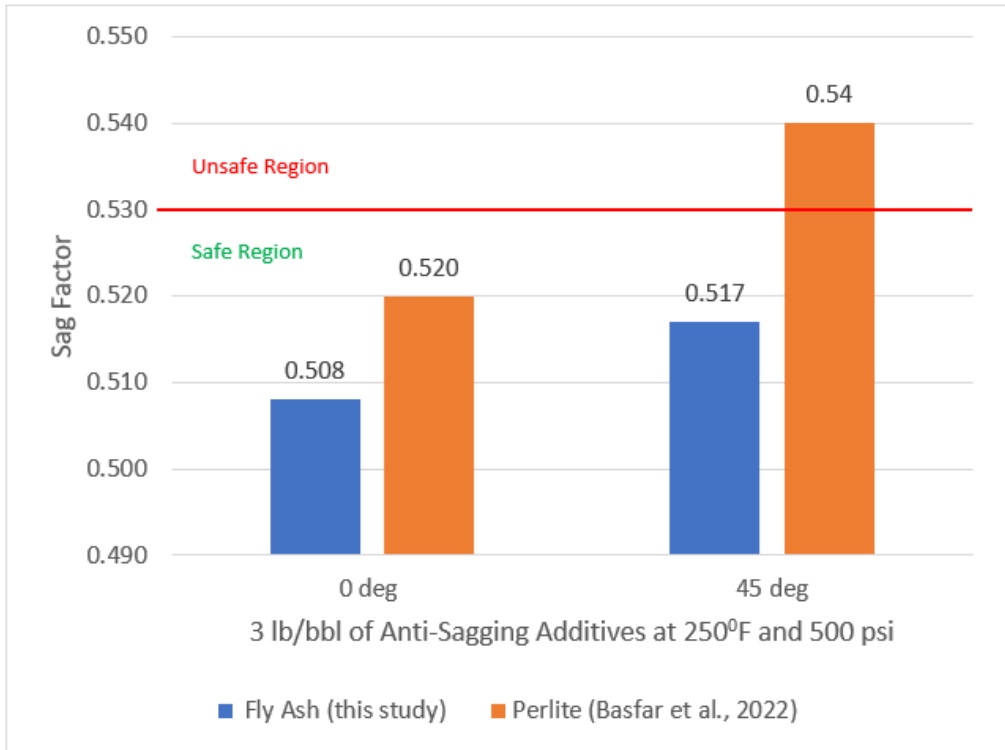


Figure 23. Static sag results comparison between fly ash (this study) and perlite (Basfar et al., 2022).

Figures 23 and 24 compare the performance of 3 lb./bbl of fly ash with perlite, at static and dynamic sag conditions respectively. The results of the efficiency of fly ash with perlite at vertical and inclined conditions were elaborated in Figure 23. An efficiency of 2% and 4% increase in static sag reduction were exhibited by fly ash over perlite at the vertical (0°) and inclined (45°) positions respectively. Figure 24 showcases a 43% increase in the percentage reduction efficiency of fly ash over perlite at dynamic conditions. Even though fly ash and perlite have similar properties like crystal shape (amorphous), and pH value (about 5 – 8 in 10% solution), perlite is slightly denser soluble in water than fly ash. The little difference in efficiency may be from the other physicochemical properties. Considering the economic aspect of anti-sagging additives, the

average cost of perlite in North Dakota, United States is about \$63/ton (USGS, 2021) while fly ash is relatively at no cost since it is an industrial waste. Deductively, fly ash may be referred to as a better anti-sagging additive than perlite.

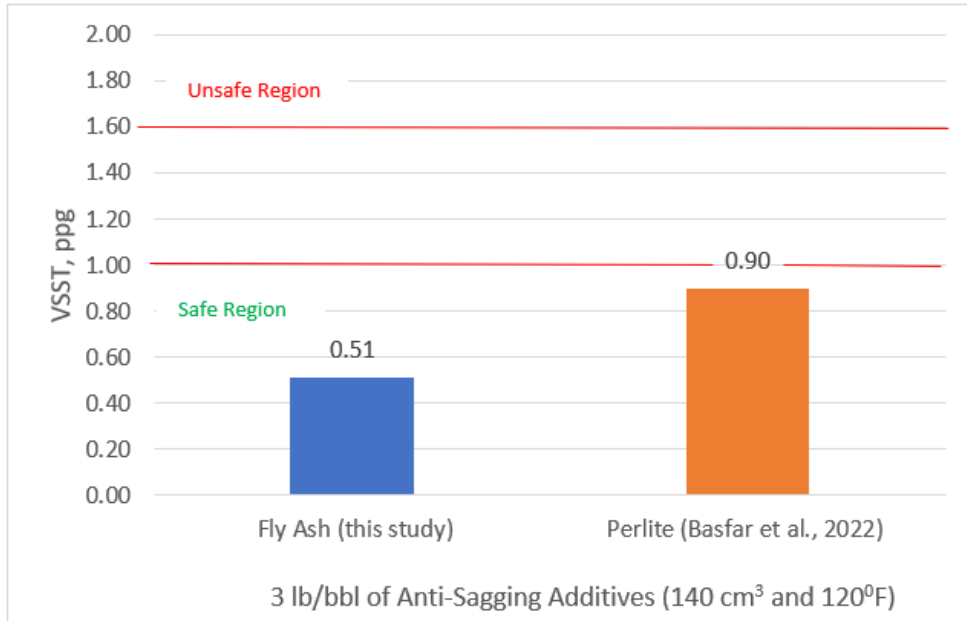


Figure 24. Dynamic sag results comparison between fly ash (this study) and perlite (Basfar et al., 2022).

For the purpose of visualization, as depicted in Figure 25, the inclined sag phenomenon may be demonstrated in the laboratory with the aid of a transparent glass measuring cylinder placed on an inclinometer. The cylinder may be a quarter filled up with a freshly agitated mud sample and topped off with water up to three-quarters. Agitate vigorously to form a homogenous sample and set it on an inclinometer at the desired angle of deviation to allow for settling. After settling, a trail of water is observed on the upper side of the tube flows upward, and the ilmenite particles roll downwards depending on the angle of deviation. At this stage, the influence of particle density comes into play, particles are segregated based on density differences. As such, fluids with low

density are pushed ascensional, while the high density is pushed down on the lower side of the borehole. Sag occurs when ilmenite particles (weight material) settle and constitute a layer of an ultra-high density viscous fluid on the low side of the borehole referred to as the settled ilmenite bed in Figure 25. However, the plunged particles are a bed of slumped ilmenite particles that rolled downward from the hanging side of the hole. The clarified mud is the settled fluid or layer of low-density fluids at the top of the hole.

Practically, sagging can be seen occurring at vertical and inclined positions, as well as in static and dynamic conditions. Static conditions may occur when the bed develops due to a no-motion situation, especially when the mud-circulating pumps are off. Slumps grow faster in this condition. Conversely, dynamic conditions occur when the flow rate is low or steady which may enhance deposition and subsequent bed formation. The weighting agent will fall out of a stationary fluid column if it is not adequately suspended. The regularity of hindered settlement in vertical wells is significantly slower than that of free settling of a single particle. The formation of the gel structure enhances suspension, and settling is reduced. However, the settling rate may be significantly increased when the column is inclined.

Table 5, is populated with results obtained for Base Mud plus 3 lb./bbl of fly ash, comparing static conditions (vertical position, 0°) with inclined position (60°). It may be inferred that free settling which occurs in the inclined position is greater than hindered settling which takes place in the vertical position. This is true for all the temperatures investigated, which may be due to the gradual increment in the surface space of the fluid in the hole. Therefore, ilmenite particles become sparsely populated. The effect of gravity on ilmenite particles is easily pronounced when particles are sparsely populated due to inadequate support to prevent settling. Eventually, the increase in surface space from the vertical position (0°) to the inclination (60°) may initiate free settling.

Ilmenite particles due to higher specific gravities have more tendencies to settle out unhindered and form sag beds on the hanging side of the wellbore. Sometimes, slumped down to the bottom-most part of the hole, shown as plunged particles in Figure 25. This may be responsible for sagging at inclined positions greater than sagging at vertical positions (Skalle et al., 1999). High temperature which degrades polymer may be a contributory factor to this. In addition, due to the large surface space possessed by inclined holes, weight materials have higher tendencies to settle out unhindered and form sag beds on the hanging side of the wellbore. Sometimes, slumped down to the bottom-most part of the hole, shown as plunged particles in Figure 25.

Table 5.

Relationship between the angles of inclination and settling.

	Static condition (Vertical position, 0°)	Static condition (Inclined position, 60°)	Free Settling (Inclined)	Hindered Settling (Vertical)
250°F	0.508	0.520	X	-
300°F	0.512	0.525	X	-
350°F	0.516	0.526	X	-
400°F	0.519	0.527	X	-

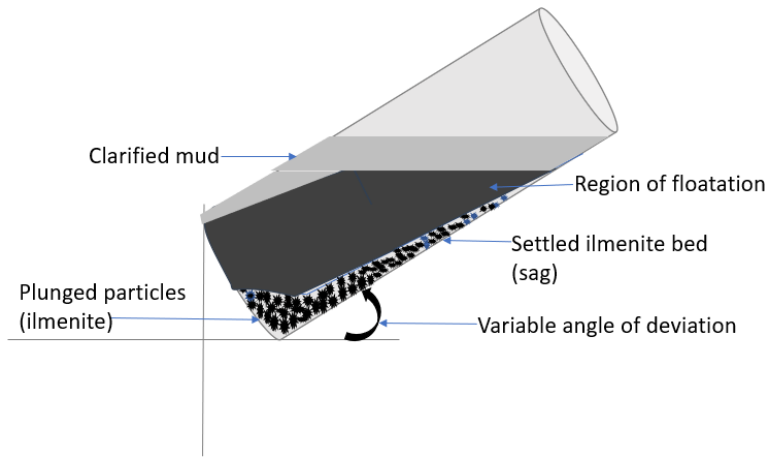


Figure 25. Schematic of an incline sag phenomenon

4.1 Rheology

The results of the flow characteristics such as 10 mins and secs gel, plastic and apparent viscosity, and yield point examined at 450⁰F, as presented validate the hole cleaning capacity, wellbore hydraulics, and stability of the drilling mud.

As seen in Figure 26, at 450⁰F, the Base Mud with 1, 2, and 3 lb./bbl of fly ash exhibited a good performance of 34 cP which is very close to the API recommended value of 35 cP for a high-performance mud. Base Mud plus 0 lb./bbl of fly ash sample gave a poor PV performance, this may cause instability due to the absence of fly ash.



Figure 26. Effect of different ratios of fly ash on PV at 450⁰F

From Figure 27, it can be deduced that the addition of a higher ratio of fly ash gave a better YP performance. The results of the YP at 450⁰F were between the API values for a high-performance mud. This is an indication of improved YP for Base Mud with 1, 2, and 3 lb./bbl of fly ash.

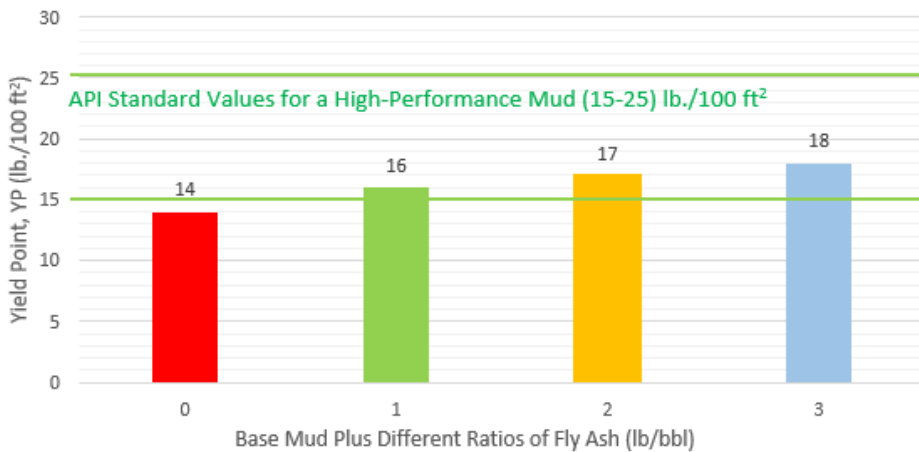


Figure 27. Effect of different ratios of fly ash on YP at 450⁰F

As observed in Figures 28 and 29, the addition of a larger quantity of fly ash may be effective in raising the gel strength of the samples, and subsequently improving the suspension capacity of the mud samples at 450⁰F. This may be a good anti-sag tendency performance, as enhanced gel structures help in preventing particle settling. On the contrary, the Base Mud plus 0 lb./bb of fly ash exhibited a lower gel strength which confirms that these samples are unstable and could sag at both static and dynamic conditions in high temperatures.

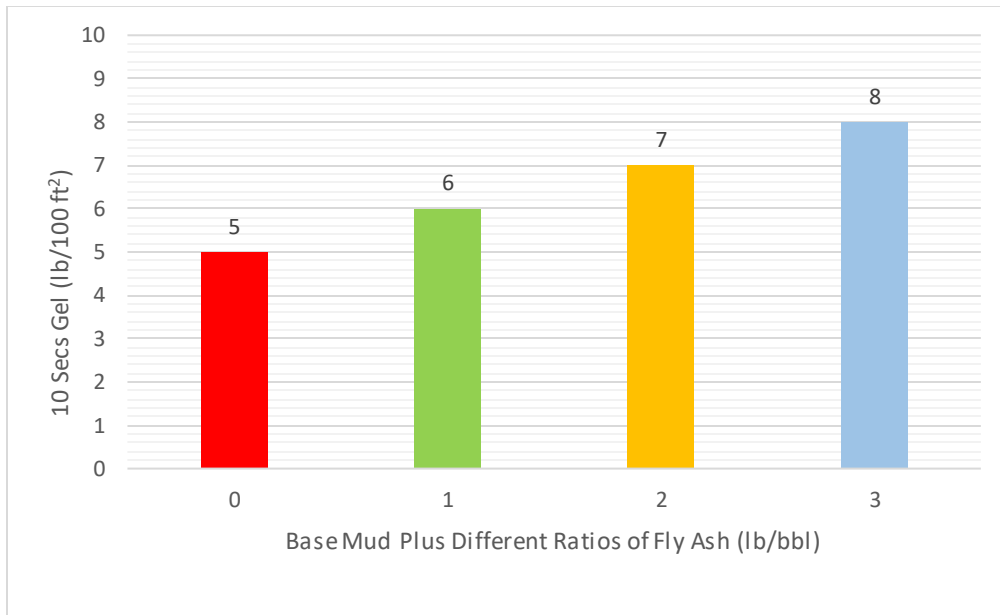


Figure 28. Effect of different ratios of fly ash on 10 secs gel at 450⁰F

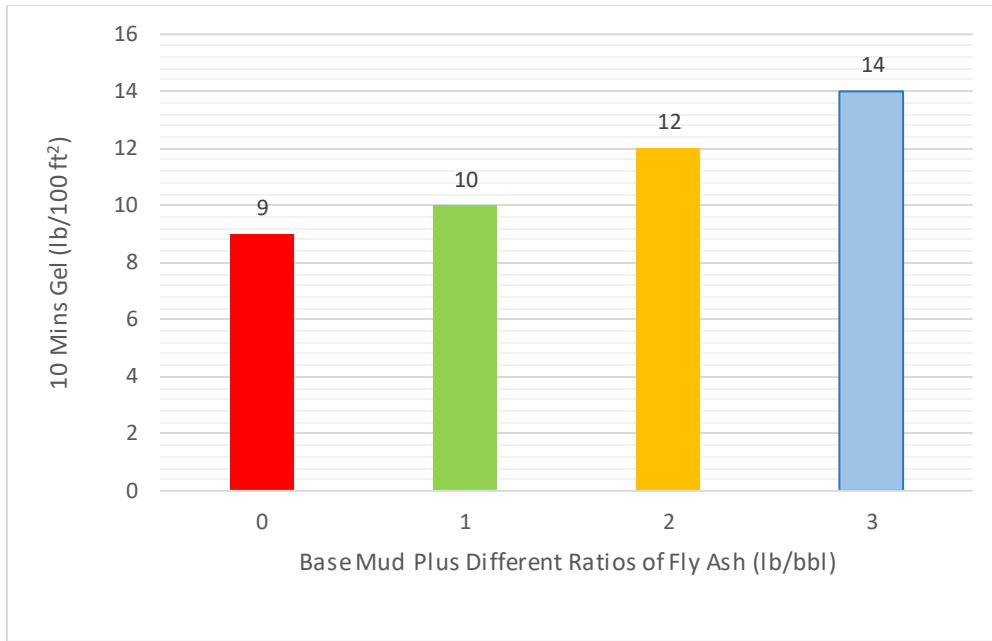


Figure 29. Effect of different ratios of fly ash on 10 mins gel at 450⁰F

4.2 Filtration Loss

Figure 30 showcases the effect of fly ash as the filtrate loss-reducing additive on the filtrate volume at varying times of the invasion. It has been demonstrated that as the weight amount of fly ash increases the filtrate volume decreases, hence reducing the permeability of the mud cake. Using the formulation in Base Mud plus 0 lb./bbl of fly ash as a benchmark, there was a notable reduction of 43%, 66%, and 73% in filtrate volume due to the influence of 1, 2, and 3 lb./bbl of fly ash respectively mixed in the three mud mixtures.

The filter cake thickness was directly measured with a caliper, and the results are shown in Figure 31. It is evident that 17.6 ml, 10.8 ml, 6.6 ml, and 4.2 ml of filtrate volume resulted in a thickness of 14.31 mm, 5.5 mm, 5.14 mm, and 5.25 mm respectively as demonstrated in Figures 30, and 31. An addition of 1 lb./bbl of fly ash into the Base Mud mixture lowered the cake's thickness from

14.31 mm to 5.5 mm (61%), while the addition of 2 lb./bbl further reduced the thickness by 64%. However, an additional increase in the concentration of fly ash to 3 lb./bbl (Base Mud plus 3 lb./bbl of fly ash) gave a 63% reduction. This depicts that fly ash can serve as a fast and efficient sealing agent during the filtrate loss process in the drilling operation.

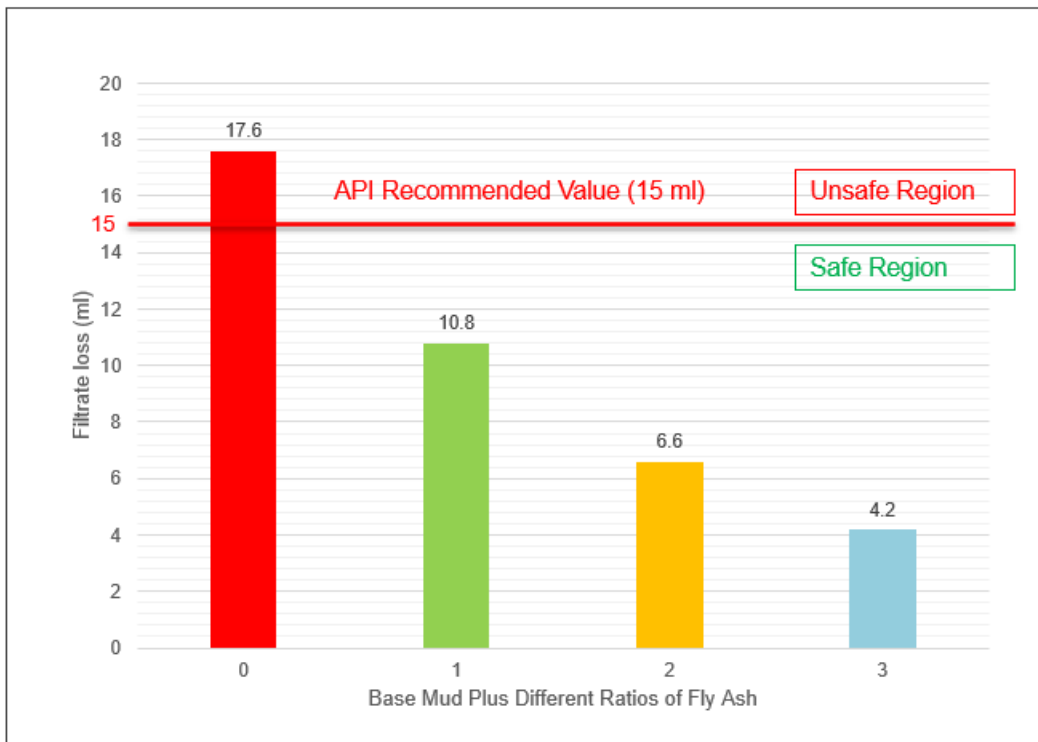


Figure 30. Filtrate loss of Base Mud plus different ratios fly ash.

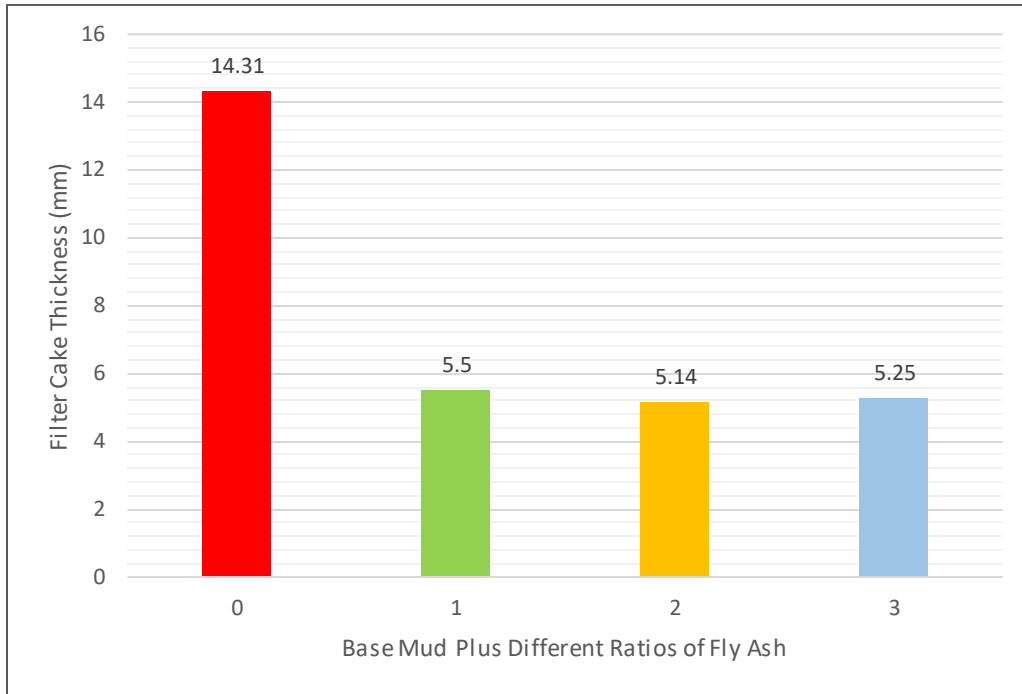


Figure 31. Filtrate cake thickness of Base Mud plus different ratios fly ash.

CHAPTER V

CONCLUSION

Fly ash's effectiveness at improving the solid-sagging, rheological, and filtration properties of a geothermal drilling fluid made of ilmenite-densified water-based mud was assessed in this study.

The next submissions were inferred:

1. At elevated temperatures ranging from 250⁰F to 400⁰F, the effectiveness of fly ash particles has been established to serve as a good sag recipe for ilmenite-densified water-based drilling fluid by reduction at both statically and dynamically sagging positions.
2. Base Mud lacking fly ash particles (0 lb./bbl of fly ash) presented a higher susceptibility to sag which is beyond the API tolerable standard of SF and VSST. The inclusion of fly ash to the based mud with a ratio of 3 lb./bbl is effective in stabilizing the mud in a highly deviated well at the temperature considered in this study and respectively reduces SF and VSST values of 1 ppg and 0.53 which are the API acceptable value for static and dynamic sagging tendency.
3. It was unveiled that the angle of hole deviation and temperature play an important role when measuring sagging tendency. The sag factor increases as the angle of inclination increases from 30° to 60° and it then decreases as the angle of inclination further increases to 90°. It has been demonstrated that the highest sag factor occurs at nearly 60° for all the temperatures investigated, where the highest sagging tendency is experienced at 400⁰F. Invariably, the higher the temperature, the higher the corresponding increase in sagging, and the highest static sag at an inclined position is expected at around 60°. In addition, due

to the larger surface area of inclined holes to vertical holes, deviated holes are prone to faster free settling of weight material.

4. An efficiency of 2% and 4% increase in static sag reduction were exhibited by fly ash over perlite at the vertical (0°) and inclined (45°) positions respectively as demonstrated in Figure 13. An increase of 43% sag reduction was also observed at dynamic conditions using fly ash over perlite as compared in Figure 14. Even though fly ash and perlite shared similar properties like crystal shape (amorphous), and pH value (about 5 – 8 in 10% solution).
5. The addition of fly ash to the mud formulation improved the flow properties; plastic viscosity, yield point, and gel strengths were improved at 450°F . Thus, enhancing the drilling mud functions.
6. Fly ash powder at a concentration of 1 lb./bbl in an Ilmenite densified water-base drilling fluid is adequate to reduce the filter cake's thickness from 17.6 ml to 10.8 ml, which is within the allowable API value. This amount was sufficient to reduce the filtration volume by 38% and the mud cake thickness by 61%. The volume and rate of filtration are only marginally lowered by adding more fly ash, while the thickness of the mud cake was further reduced by 64% (Mud 2).
7. An improvement of 64% decrease in cake thickness observed for fly ash was a result of higher efficiency. This supports the critical function fly ash plays in lowering filter cake thickness.

REFERENCES

- Abdou, M. I., Al-Sabagh, A. M., Ahmed, H. E. S., & Fadl, A. M. (2018). Impact of barite and ilmenite mixture on enhancing the drilling mud weight. *Egyptian Journal of Petroleum*, 27(4), 955-967. <https://doi.org/10.1016/j.ejpe.2018.02.004>
- Afroz, S., Zhang, Y., Nguyen, Q. D., Kim, T., & Castel, A. (2023). Shrinkage of blended cement concrete with fly ash or limestone calcined clay. *Materials and Structures*, 56(1), 15.
- Ahmad, H. M., Kamal, M. S., & Al-Harhi, M. A. (2018). High molecular weight copolymers as rheology modifier and fluid loss additive for water-based drilling fluids. *Journal of Molecular Liquids*, 252, 133-143. <https://doi.org/10.1016/j.molliq.2017.12.135>
- Ahmaruzzaman, M. (2010). A review on the utilization of fly ash. *Progress in energy and combustion science*, 36(3), 327-363.
- Ahmed, A., Alsaihati, A., & Elkatatny, S. (2021). An overview of the common water-based formulations used for drilling onshore gas wells in the Middle East. *Arabian Journal for Science and Engineering*, 46, 6867-6877. <https://link.springer.com/article/10.1007/s13369-020-05107-z>
- Ahmed, A., Basfar, S., Elkatatny, S., & Bageri, B. (2022). Vermiculite for enhancement of barite stability in water-based mud at elevated temperature. *Powder Technology*, 401, 117277. <https://doi.org/10.1016/j.powtec.2022.117277>
- Al-Abdullatif, Z., Al-Yami, A., Wagle, V., Bubshait, A., & Al-Safran, A. (2014, November). Development of new kill fluids with minimum sagging problems for high pressure Jilh formation in Saudi Arabia. In *Abu Dhabi International Petroleum Exhibition and Conference*. OnePetro. <https://doi.org/10.2118/171683-MS>

Al-Bagoury, M. (2014, April). Micronized Ilmenite-A non-damaging & non-sagging new weight material for drilling fluids. In *SPE Bergen One Day Seminar*. OnePetro. <https://doi.org/10.2118/169182-MS>

Aldea, C., Growcock, F. B., Lee, L. J., Friedheim, J. E., & Van Oort, E. (2001, March). Prevention of dynamic sag in deepwater invert emulsion fluids. In *Proceedings of the AADE 2001 National Drilling Conference, 'Drilling Technology', Houston, TX, USA* (pp. 27-29).

Al-Hameedi, A. T. T., Alkinani, H. H., Dunn-Norman, S., Al-Alwani, M. A., Alshammari, A. F., Albazzaz, H. W., ... & Mutar, R. A. (2019). Insights into the application of new eco-friendly drilling fluid additive to improve the fluid properties in water-based drilling fluid systems. *Journal of Petroleum Science and Engineering*, 183, 106424. <https://doi.org/10.1016/j.petrol.2019.106424>

Al-Yami, A. S., Nasr-El-Din, H. A., Al-Majed, A. A., & Menouar, H. (2007, November). An innovative manganese tetra-oxide/KCl water-based drill-in fluids for HT/HP wells. In *SPE Annual Technical Conference and Exhibition*. OnePetro. <https://doi.org/10.2118/110638-MS>

Amani, M., & Al-Jubouri, M. (2012). The effect of high pressures and high temperatures on the properties of water based drilling fluids. *Energy Science and Technology*, 4(1), 27-33. [I:10.3968/j.est.1923847920120401.256](https://doi.org/10.3968/j.est.1923847920120401.256)

Amani, M., & Al-Jubouri, M. (2012, September). An experimental investigation of the effects of ultra-high pressure and temperature on the rheological properties of water-based drilling fluids. In *International Conference on Health, Safety and Environment in Oil and Gas Exploration and Production*. OnePetro. <https://doi.org/10.2118/157219-MS>

Amighi, M. R., & Shahbazi, K. (2010, January). Effective ways to avoid barite sag and technologies to predict sag in HPHT and deviated wells. In *SPE Deep Gas Conference and Exhibition*. OnePetro.

Avci, E., & Mert, B. A. (2019). The rheology and performance of geothermal spring water-based drilling fluids. *Geofluids*, 2019. <https://doi.org/10.1155/2019/3786293>

Bageri, B. S., Benaafi, M., Mahmoud, M., Patil, S., Mohamed, A., & Elkatatny, S. (2019). Effect of arenite, calcareous, argillaceous, and ferruginous sandstone cuttings on filter cake and drilling fluid properties in horizontal wells. *Geofluids*, 2019. <https://doi.org/10.1155/2019/1956715>

Bageri, B. S., Mahmoud, M., Elkatatny, S., Patil, S., Benaafi, M., & Mohamed, A. (2019, June). Effect of drill cuttings mechanical properties on filter cake properties and mud-filtrate invasion. In *ARMA US Rock Mechanics/Geomechanics Symposium* (pp. ARMA-2019). ARMA. <https://onepetro.org/ARMAUSRMS/proceedings/ARMA19/All-ARMA19/ARMA-2019-1662/124878>

Bageri, B. S., Adebayo, A. R., Al Jaber, J., & Patil, S. (2020a). Effect of perlite particles on the filtration properties of high-density barite weighted water-based drilling fluid. *Powder Technology*, 360, 1157-1166. <https://doi.org/10.1016/j.powtec.2019.11.030>

Bageri, B. S., Benaafi, M., Mahmoud, M., Mohamed, A., Patil, S., & Elkatatny, S. (2020b). Effect of formation cutting's mechanical properties on drilling fluid properties during drilling operations. *Arabian Journal for Science and Engineering*, 45, 7763-7772. <https://link.springer.com/article/10.1007/s13369-020-04424-7>

Basfar, S., Elkatatny, S., Mahmoud, M., Kamal, M. S., Murtaza, M., & Stanitzek, T. (2018, April). Prevention of barite sagging while drilling high-pressure high-temperature (HPHT) wells. In *SPE*

Kingdom of Saudi Arabia Annual Technical Symposium and Exhibition. OnePetro.
<https://doi.org/10.2118/192198-MS>

Basfar, S., Mohamed, A., Elkatatny, S., & Al-Majed, A. (2019). A combined barite–ilmenite weighting material to prevent barite sag in water-based drilling fluid.
<https://doi.org/10.3390/ma12121945>

Basfar, S., Ahmed, A., & Elkatatny, S. (2021). Stability enhancing of water-based drilling fluid at high pressure high temperature. *Arabian Journal for Science and Engineering*, 46, 6895-6901.
<https://link.springer.com/article/10.1007/s13369-020-05126-w>

Bern, P. A., van Oort, E., Neustadt, B., Ebeltoft, H., Zurdo, C., Zamora, M., & Slater, K. S. (2000). Barite sag: measurement, modeling, and management. *SPE Drilling & Completion*, 15(01), 25-30.
<https://doi.org/10.2118/62051-PA>

Bern, P. A., Zamora, M., Hemphill, A. T., Marshall, D., Omland, T. H., & Morton, E. (2010, April). Field monitoring of weight-material sag. In *2010 AADE Fluids Conference and Exhibition*.
<https://www.aade.org/application/files/3415/7261/7999/AADE-10-DF-HO-25.pdf>

Boyou, N. V., Ismail, I., Sulaiman, W. R. W., Haddad, A. S., Husein, N., Hui, H. T., & Nadaraja, K. (2019). Experimental investigation of hole cleaning in directional drilling by using nano-enhanced water-based drilling fluids. *Journal of Petroleum Science and Engineering*, 176, 220-231. <https://doi.org/10.1016/j.petrol.2019.01.063>

Blomberg, N. E., & Melberg, B. (1984). Evaluation of ilmenite as weight material in drilling fluids. *Journal of petroleum technology*, 36(06), 969-974. <https://doi.org/10.2118/11085-PA>

Caenn, R., Darley, H. C., & Gray, G. R. (2011). *Composition and properties of drilling and completion fluids*. Gulf professional publishing.

Chilingarian, G. V., Alp, E., Caenn, R., Al-Salem, M., Uslu, S., Gonzales, S., ... & Yen, T. F. (1986). Drilling fluid evaluation using yield point-plastic viscosity correlation. *Energy sources*, 8(2-3), 233-244

Davis, C. L., Livanec, P. W., & Shumway, W. W. (2020). *U.S. Patent No. 10,590,323*. Washington, DC: U.S. Patent and Trademark Office.

Davison, J. M., Jones, M., Shuchart, C. E., & Gerard, C. (2001). Oil-based muds for reservoir drilling: their performance and cleanup characteristics. *SPE Drilling & Completion*, 16(02), 127-134. <https://doi.org/10.2118/72063-PA>

Elkatatny, S. M., Al Moajil, A., & Nasr-El-Din, H. A. (2012, July). Evaluation of a new environmentally friendly treatment to remove Mn₃O₄ filter cake. In *IADC/SPE Asia Pacific Drilling Technology Conference and Exhibition*. OnePetro. <https://doi.org/10.2118/156451-MS>

Elkatatny, S. M., Nasr-El-Din, H. A., & Al-Bagoury, M. (2012, December). Evaluation of micronized ilmenite as weighting material in water-based drilling fluids for HPHT applications. In *SPE Kuwait International Petroleum Conference and Exhibition*. OnePetro. <https://doi.org/10.2118/163377-MS>

Elkatatny, S. (2018). Enhancing the stability of invert emulsion drilling fluid for drilling in high-pressure high-temperature conditions. <https://doi.org/10.3390/en11092393>

Elkatatny, S. (2019). Mitigation of barite sagging during the drilling of high-pressure high-temperature wells using an invert emulsion drilling fluid. *Powder technology*, 352, 325-330.

<https://doi.org/10.1016/j.powtec.2019.04.037>

Fattah, K. A., & Lashin, A. (2016). Investigation of mud density and weighting materials effect on drilling fluid filter cake properties and formation damage. *Journal of African Earth Sciences*, 117, 345-357.

<https://doi.org/10.1016/j.jafrearsci.2016.02.003>

Gray, G. R., & Young Jr, F. S. (1973). 25 years of drilling technology-a review of significant accomplishments. *Journal of Petroleum Technology*, 25(12), 1347-1354.

<https://doi.org/10.2118/4700-PA>

Haaland, E., Pettersen, G., & Tuntland, O. B. (1976). Testing of iron oxides as weight materials for drilling muds. *paper SPE*, 6218.

Hanson, P. M., Trigg Jr, T. K., Rachal, G., & Zamora, M. (1990, September). Investigation of barite" sag" in weighted drilling fluids in highly deviated wells. In *SPE Annual Technical Conference and Exhibition?* (pp. SPE-20423). SPE.

<https://doi.org/10.2118/20423-MS>

Hossain, M. E., & Al-Majed, A. A. (2015). *Fundamentals of sustainable drilling engineering*. John Wiley & Sons.

Jefferson, D. T. (1991). New procedure helps monitor sag in the field. *paper ASME*, 91, 20-24.

Mahmoud, M., Abdulraheem, A., Al-Mutairi, S. H., Elkatatny, S. M., & Shawabkeh, R. A. (2017).

Single stage filter cake removal of barite weighted water based drilling fluid. *Journal of Petroleum Science and Engineering*, 149, 476-484.<https://doi.org/10.1016/j.petrol.2016.10.059>

Maxey, J. (2007). Rheological analysis of static and dynamic sag in drilling fluids. *Annual Transactions-Nordic Rheology Society*, 15, 181.

Medhi, S., Gupta, D. K., & Sangwai, J. S. (2021). Impact of zinc oxide nanoparticles on the rheological and fluid-loss properties, and the hydraulic performance of non-damaging drilling fluid. *Journal of Natural Gas Science and Engineering*, 88, 103834. <https://doi.org/10.1016/j.jngse.2021.103834>

Mohamed, A. K., Elkatatny, S. A., Mahmoud, M. A., Shawabkeh, R. A., & Al-Majed, A. A. (2017, March). The evaluation of micronized barite as a weighting material for completing HPHT wells. In *SPE Middle East Oil & Gas Show and Conference*. OnePetro. <https://doi.org/10.2118/183768-MS>

Mohamed, A., Basfar, S., Elkatatny, S., & Al-Majed, A. (2019). Prevention of barite sag in oil-based drilling fluids using a mixture of barite and ilmenite as weighting material. *Sustainability*, 11(20), 5617.

Mohamed, A., Al-Afnan, S., Elkatatny, S., & Hussein, I. (2020). Prevention of barite sag in water-based drilling fluids by a urea-based additive for drilling deep formations. *Sustainability*, 12(7), 2719. <https://doi.org/10.3390/su12072719>

Murphy, R., Jamison, D., Hemphill, T., Bell, S., Albrecht, C. (2008). Measuring and predicting dynamic sag. *SPE Drill Complete* 23(02):142–149. <https://doi.org/10.2118/103088-PA>

Mushtaq, F., Zahid, M., Bhatti, I. A., Nasir, S., & Hussain, T. (2019). Possible applications of coal fly ash in wastewater treatment. *Journal of environmental management*, 240, 27-46. <https://doi.org/10.1016/j.jenvman.2019.03.054>

- Nguyen, T., Miska, S., Yu, M., & Takach, N. (2011). Predicting dynamic barite sag in newtonian-oil based drilling fluids in pipe. *Journal of energy resources technology*, 133(2). <https://doi.org/10.1115/1.4004026>
- Ofei, T. N., Lund, B., Saasen, A., Sangesland, S., Linga, H., Gyland, K. R., & Kawaji, M. (2020, February). Barite sag measurements. In *IADC/SPE International Drilling Conference and Exhibition*. OnePetro. <https://doi.org/10.2118/199567-MS>
- Omland, T. H., Saasen, A., Van Der Zwaag, C., & Amundsen, P. A. (2007, October). The effect of weighting material sag on drilling operation efficiency. In *Asia Pacific Oil and Gas Conference and Exhibition*. OnePetro. <https://doi.org/10.2118/110537-MS>
- Perween, S., Thakur, N. K., Beg, M., Sharma, S., & Ranjan, A. (2019). Enhancing the properties of water-based drilling fluid using bismuth ferrite nanoparticles. *Colloids and Surfaces A: Physicochemical and Engineering Aspects*, 561, 165-177. <https://doi.org/10.1016/j.colsurfa.2018.10.060>
- Power, D., & Zamora, M. (2003, April). Drilling fluid yield stress: measurement techniques for improved understanding of critical drilling fluid parameters. In *AADE Technical Conference, Houston* (Vol. 2003, pp. 1-3). <https://www.aade.org/application/files/7515/7304/4604/AADE-03-NTCE-35-Power.pdf>
- Pozebon, D., Lima, E. C., Maia, S. M., & Fachel, J. M. (2005). Heavy metals contribution of non-aqueous fluids used in offshore oil drilling. *Fuel*, 84(1), 53-61. <https://doi.org/10.1016/j.fuel.2004.08.002>

Saasen, A., Liu, D., Marken, C. D., Sterri, N., Halsey, G. W., & Isambourg, P. (1995, February). Prediction of barite sag potential of drilling fluids from rheological measurements. In *SPE/IADC Drilling Conference and Exhibition* (pp. SPE-29410). SPE. <https://doi.org/10.2118/29410-MS>

Saasen, A., Jordal, O. H., Burkhead, D., Berg, P. C., Løklingholm, G., Pedersen, E. S., ... & Harris, M. J. (2002, February). Drilling HT/HP wells using a cesium formate based drilling fluid. In *IADC/SPE Drilling Conference*. OnePetro. <https://doi.org/10.2118/74541-MS>

Scott, P. D., Zamora, M., & Aldea, C. (2004, March). Barite-sag management: challenges, strategies, opportunities. In *IADC/SPE Drilling Conference*. OnePetro. <https://doi.org/10.2118/87136-MS>

Singh, N. B., Agarwal, A., De, A., & Singh, P. (2022). Coal fly ash: An emerging material for water remediation. *International Journal of Coal Science & Technology*, 9(1), 44.

Skalle, P., Backe, K. R., Lyomov, S. K., & Sveen, J. (1999). Barite segregation in inclined boreholes. *Journal of Canadian Petroleum Technology*, 38(13). <https://doi.org/10.2118/99-13-11>

Stroud, B. K. (1926). *U.S. Patent No. 1,575,945*. Washington, DC: U.S. Patent and Trademark Office.

Wagle, V., Maghrabi, S., & Kulkarni, D. (2013, March). Formulating sag-resistant, low-gravity solids-free invert emulsion fluids. In *SPE Middle East Oil and Gas Show and Conference*. OnePetro. <https://doi.org/10.2118/164200-MS>

Wagle, V., Al-Yami, A. S., & AlAbdullatif, Z. (2015, March). Using nanoparticles to formulate sag-resistant invert emulsion drilling fluids. In *SPE/IADC Drilling Conference and Exhibition*. OnePetro. <https://doi.org/10.2118/173004-MS>

Teixeira, E. R., Camões, A., Branco, F. G., Aguiar, J. B., & Figueiro, R. (2019). Recycling of biomass and coal fly ash as cement replacement material and its effect on hydration and carbonation of concrete. *Waste Management, 94*, 39-48.

Temple, C., Paterson, A. F., & Leith, C. D. (2005). *U.S. Patent No. 6,861,393*. Washington, DC: U.S. Patent and Trademark Office.

Tehrani, A., Cliffe, A., Hodder, M. H., Young, S., Lee, J., Stark, J., & Seale, S. (2014, March). Alternative drilling fluid weighting agents: a comprehensive study on ilmenite and hematite. In *IADC/SPE Drilling Conference and Exhibition*. OnePetro. <https://doi.org/10.2118/167937-MS>

Teodoriu, C. (2015, April). Why and when does casing fail in geothermal wells: a surprising question. In *Proceedings of the world geothermal congress*.

Vivas, C., Salehi, S., Tuttle, J. D., & Rickard, B. (2020). Challenges and opportunities of geothermal drilling for renewable energy generation. *GRC Transactions, 44*, 904-918.

Yao, R., Jiang, G., Li, W., Deng, T., & Zhang, H. (2014). Effect of water-based drilling fluid components on filter cake structure. *Powder technology, 262*, 51-61. <https://doi.org/10.1016/j.powtec.2014.04.060>

Tillotson, S. J. (2002, April). North Dakota Regulatory Perspective. In *Coal Combustion By-Products and Western Coal Mines: A Technical Interactive Forum* (p. 257). <https://citeseerx.ist.psu.edu/document?repid=rep1&type=pdf&doi=24fe87df3fa820f5c62a838dba-be0788acfldd41#page=250>

Tuntland, O. B., Herfjord, H. J., Lehne, K. A., & Haaland, E. (1981). Iron oxides as weight materials for drilling mud. *Erdoel-Erdgas Z.;*(Germany, Federal Republic of), 97(8).

<https://www.osti.gov/etdeweb/biblio/5832121>

Zamora, M., & Bell, R. (2004, April). Improved wellsite test for monitoring barite sag. In *proceedings of the AADE 2004 drilling fluids conference, Houston, TX, USA* (pp. 6-7).

<https://www.aade.org/application/files/6315/7295/4830/AADE-04-DF-HO-19.pdf>

Xiao, J., Nasr-El-Din, H. A., & Al-Bagoury, M. (2013, June). Evaluation of micronized ilmenite as a weighting material in oil-based drilling fluids for HPHT applications. In *SPE European Formation Damage Conference & Exhibition*. OnePetro. <https://doi.org/10.2118/165184-MS>